Bull. Mater. Sci. Vol. 4, No. 5, December 1982, pp. 483–526. © Printed in India.

Semiconductor based photoelectrochemical cells for solar energy conversion—An overview

A ARUCHAMY, G ARAVAMUDAN and G V SUBBA RAO
Materials Science Research Centre, Indian Institute of Technology, Madras 600 036, India

MS received 1 December 1981

Abstract. An overview of the semiconductor based photoelectrochemical (PEC) cells for solar energy conversion is presented. PEC cells are of two types: photoelectrolysis cells and photovoltaic cells. The principles involved, electrode and electrode/electrolyte interface characteristics, experimental methods of investigation and energy conversion efficiency are discussed in detail. Up-to-date data on various PEC cells are also presented and discussed.

Keywords. Photoelectrochemical (PEC) cells; solar energy conversion; semiconductor photoelectrochemistry; energy conversion efficiency.

1. Introduction

Solar energy as available on the surface of the earth constitutes clean, non-polluting, abundant and relatively 'free' energy source. As much solar energy falls on earth's surface in a fortnight as the energy contained in the world's fossil fuel sources (10^{16} kW). The mean solar irradiance at normal incidence outside the atmosphere is 1360 W/m^2. Total annual incidence of solar energy in India is about 10^7 kW and for the southern region the daily average is 0·4 kW/m^2. The solar radiation occupies the electromagnetic spectral range 2000–20000 Å. Forty-five percent of this spectral energy is distributed in the visible region, 52% in the near IR and the rest in the UV and far IR regions. However, this spectral distribution of sunlight reaching the earth's surface is modified (and the intensity reduced) due to atmospheric extinction and selective absorption by CO_2, O_3 and water vapour and scattering due to clouds, dust and water droplets. Thus, solar radiation on earth is either direct or diffused depending on the path length and transparency of the atmosphere. On clear days, about 90% is direct radiation and the rest is diffused.

There are various ways of tapping the solar energy for useful purposes. The simplest one is the solar heat collector, (*e.g.*, a 'selective' black surface under a pane of glass and other similar variations) and can absorb all portions of the solar spectrum. Various practical devices based on the solar collectors are known. On the other hand, direct systems which convert radiant energy to electrical energy (*e.g.*, solid state Si photovoltaic solar cell) or chemical energy (*e.g.*, as H_2 gas in a photoelectrolysis cell) can generally use only the higher energy portion of the solar spectrum. This is because the direct transmutation devices are quantum converters, in which a photon of light is absorbed and causes an electron-hole pair to be produced or a chemical bond to break in a semiconducting crystal. Such processes can only be induced by relatively energetic photons of wavelength λ in the range 2000–10000 Å (6–1·2 eV), and the considerable IR portion of sunlight cannot be used. In addition to the wavelength dependence of direct converters, we have also to take the intensity (flux density of light quanta) of the solar radiation to obtain the total conversion efficiency.

Various direct radiant energy conversion devices are listed in table 1. Silicon solar cell device technology is well established except for the prohibitive cost for large scale utilization. Amorphous Si solar cells are in the developmental stage at present. The other three devices are mainly metal or semiconductor-electrolyte based systems. The photogalvanic dye-cell [cell (5) in table 1] does not employ a semiconductor (SC) electrode and hence we will not elaborate on this system. The systems of our interest are photoelectrochemical cells (PEC's) based on SC/electrolyte junction and these will be discussed below.

Semiconductor-based photoelectrochemical cells (PEC's) have come to be regarded as an important class of solar energy conversion systems. They offer a simple and efficient means for converting light into electricity or chemical energy of a fuel. Solar light to electrical or chemical energy conversion efficiencies η as high as 12% have been realized in these cells. The study of PEC's gained momentum with the first report of Fujishima and Honda (1972) concerning the photoelectrochemical decomposition of water at the *n*-type TiO_2 electrode illuminated with ultraviolet radiation. Gerischer (1975) proposed the use of PEC's for solar to electricity conversion using reversible redox systems as the electrolytes. While photoelectrolysis of water with semiconductor electrodes has met with severe materials problems, remarkable progress has been made in the area of optical-to-electricity conversion *via* PEC's in the past 4–5 years. Reviews by Nozik (1978), Harris and Wilson (1978), Tomkiewicz and Fay (1979), Butler and Ginley (1980), Rajeshwar *et al* (1978) and Gerischer (1979) summarize the findings.

A PEC is a device in which one or both the electrodes is a photoresponsive semiconductor (SC) such that irradiation of the SC with light of $h\nu \geqslant E_g$, the band gap of the SC, results in the flow of current in the external circuit (figure 1a). The photoeffect responsible for the current flow occurs at the semiconductor/electrolyte interface in which light absorption takes place in the SC to produce excess charge carriers. Effective separation of the photo-produced holes and electrons by the electric field within the SC, as discussed in detail later, is a crucial step in the photoelectrochemical process. The utilization of these cells for energy conversion depends on the understanding of the processes occurring

Table 1. Solar energy conversion devices—state of the art

Device	Example	Function and η[a]	Remarks
1. Solid state p–n junction	Si ; GaAs ; n-CdS/p-Cu_2S	Optical-to-electrical ; $\eta \sim$ 12–22% (22–30%)[b]	Technology well developed with single crystal Si solar cells ; high cost per unit energy. Amorphous Si and large grain GaAs and $Ga_{1-x}Al_xAs$ solar cells under investigation. CdS–Cu_2S cells are cheap but technology not yet well developed.
2. Schottky barrier (Metal/sc junction) and MOS (metal-oxide-sc) cells	Au/n-GaAs	Optical-to-electrical; $\eta \sim$ 9–12% (—)[b]	Usually below the efficiency of p–n cells and technology is yet to be developed.
3. Photoelectrolysis cells	(i) $SrTiO_3$/NaOH/Pt (ii) Pt/HCl/p-InP (Ru)	Optical-to-chemical (H_2) ; $\eta \sim$ 1% for (i) 12% for (ii) (20–30%)[b]	First proposed in 1972. Cell with p-InP reported in 1981 represents a significant breakthrough. Long-term stability and scaling-up problems to be solved (see text).
4. sc/liquid junction solar cells or electrolyte solar cells	n-GaAs/K_2Se–K_2Se_2–KOH/C ; C/VCl_2–VCl_3/p-InP ; n-WSe_2/KI–I_2/Pt	Optical-to-electrical $\eta \sim$ 11–14% (25–30%)[b]	First proposed in 1975, breakthrough with low band gap sc's and 'suitable' redox couples (1978–81). Cheaper materials and scaling-up problems to be solved (see text).
5. Photogalvanic cells	Pt (or SnO_2)/$Fe^{2+/3+}$, thionine leuco-thionine/Pt and similar redox-dye systems	Optical-to-electrical; $\eta \sim$ 0·03% (18%)[c]	Based on redox reactions in solution under illum. and charge-transfer to inert electrodes (light absorbed by the dye molecules in solution). η is very small (back electron transfer, dye degradation, etc., reduce η). Use of more stable dyes and sc's replacing metal electrodes may offer scope for improving η. Extensive research needed.

[a] η is the max. power conversion efficiency achieved for terrestrial solar energy. Values in brackets indicate theoretically attainable upper limits considering sc's with various band gaps, including Si.

[b] see Bachman (1977) ; Gerischer (1977) ; Sze (1969).

[c] see Albery and Foulds (1979).

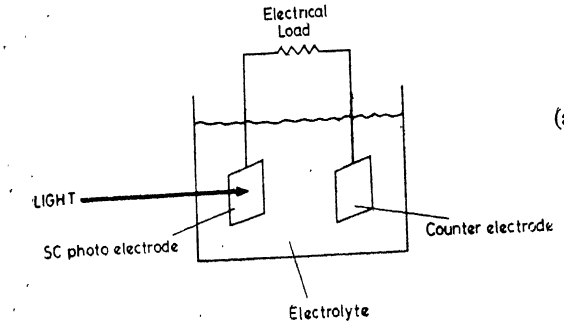

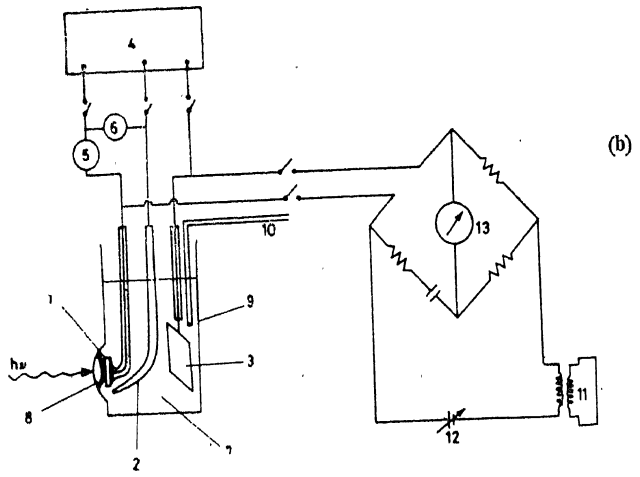

Figure 1. a. Schematic representation of a photoelectrochemical cell (PEC). b. Standard 3-electrode set-up for current-voltage (i-v) and capacitance (C) measurements. 1. Semiconductor (SC) electrode. 2. Saturated calomel electrode (SCE). 3. Platinum (counter) electrode. 4. Potentiostat. 5. Ammeter. 6. D.C. voltmeter. 7. Electrolyte. 8. Optical window for illumination of the SC photoelectrode. 9. Glass cell. 10. Gas bubbler. 11. Oscillator. 12. power supply. 13. Null detector.

inside the SC on absorption of light and the charge transfer (electrochemical) reactions that take place at the surface of the SC in contact with the electrolyte. A great deal of fundamental research into the properties of SC/electrolyte interfaces has been done over the past many years (table 2) and the essential features of most charge-transfer processes are now well understood. The contributions to the theory during this period made by Garrett and Brattain, Gerischer, Memming, Williams, Body and others led to the development of a model for SC/electrolyte interface. Although the first observation of photoeffect at the SC/electrolyte junction was reported by Becquerel (1839) it was not until very recently the use of this effect was realized for energy conversion applications. Following the work of Fujishima and Honda (1972) extensive investigations began in various aboratories. Research during the past decade has shown a lot of progress in the understanding and utilization of these cells and opened up new areas for

fundamental research. A historical account of the field of semiconductor electrochemistry is given in table 2.

Table 2. Historical account of semiconductor photoelectrochemistry

Nature of study (1)	References (2)
First observation of photo effect at silver halide electrodes in aq. solns.	Becquerel (1839)
Beginning of SC electrochemistry—study of elemental sc's (Si, Ge)	Brattain and Garrett (1955)
First comprehensive experimental studies on CdS, CdSe and other binary SC's	Williams (1960)
Development of models for SC/electrolyte interface energetics	Green (1959) ; Myamlin and Pleskov (1967) ; Gerischer (1970)
Ability of TiO_2 to oxidize water under reverse bias conditions	Body (1968)
Report of the first photoelectrolysis cell to decompose water using TiO_2 photoanode and UV radiation	Fujishima and Honda (1972)
Concept of SC/liquid junction or electrolyte solar cell	Gerischer (1975)
$SrTiO_3$—the first SC to photoelectrolyse water without externally applied bias voltage	Wrighton *et al* (1976) ; Mavroides *et al* (1975, 1976, 1978) ; Watanabe *et al* (1976)
Concept of *p–n* photoelectrolysis cells	Yeneyama *et al* (1975) ; Nozik (1976, 1977) ; Ohashi *et al* (1977a)
Study of SC's in nonaqueous solvents	Frank and Bard (1975)
Stable SC/liquid junction solar cells based on CdX (X = S, Se, Te) and aq. polychalcogenide electrolytes	Ellis *et al* (1976) ; Hodes *et al* (1976); Miller and Heller (1976)
Visible light sensitization of large band gap oxides by doping with transition metal ions	Ghosh and Maruska (1977)
Layered dichalcogenide SC's for PEC's	Tributsch *et al* (1977)
Importance of thermodynamic and kinetic considerations	Gerischer (1977) ; Bard and Wrighton (1977)
Chemical derivatization of SC electrode surfaces	Wrighton *et al* (1978)

Table 2—*Contd*

(1)	(2)
High efficiency (12%) GaAs/liquid junction solar cells (SC surface modified by Ru^{3+} ion adsorption)	Parkinson *et al* (1978a, b)
High efficiency thin film electrodes in PEC's	Heller *et al* (1979) Hodes (1980)
Effect of surface states—concept of Fermi level pinning and inversion layer model	Bard *et al* (1980); Wrighton *et al* (1980); Kautek and Gerischer (1980); Turner *et al* (1980)
High efficiency (11·5%) *p*-InP SC/liquid junction solar cell	Heller *et al* (1981)
High efficiency (12%) *p*-InP based solar photoelectrolysis cell (H_2 generation)	Heller and Vadimsky (1981)

2. The semiconductor/electrolyte interface

2.1. *Interface energetics*

The SC/electrolyte interface energetics have been dealt with in detail by Gerischer (1970). Essential features of the interface model are summarized in the following. When a SC whose Fermi level (or eletrochemical potential)* is E_F is brought into contact with an electrolyte whose electrochemical (redox) potential is E^0, an equilibrium of the electrochemical potentials of the two phases is established by transfer of electrons across the interface. This leads to a potential barrier for the further flow of charge carriers. The SC electronic bands near the surface are bent due to the depletion of majority charge carriers near the surface. The magnitude or the height of the potential barrier (also the extent of band bending), E_B, is equal to the difference in the electrochemical potentials (Fermi levels) of the two phases (SC and electrolyte) before coming into contact, given by

$$E_B = | (E_F - E^0) |. \tag{1}$$

This situation is analogous to that prevailing at a SC/metal (solid state) Schottky barrier contact. For an *n*-type SC the situations before and after contacting a metal or electrolyte are given in figure 2. The above equilibrium process gives rise to a space charge or depletion layer (depleted of the charge carriers) inside the SC, across which the potential gradient exists. The width of the depletion layer (W) is significantly larger than the Helmholtz double layer on the solution side of the interface due to smaller carrier densities inside the SC. W is usually of the order of a few thousand angstrom units. This means, the variation of field strength in the depletion layer is much smaller. The potential across the Helmholtz layer is mostly independent of the externally applied potential and

* Fermi level is same as the electrochemical potential of a semiconductor or an electrolyte nd used interchangeably.

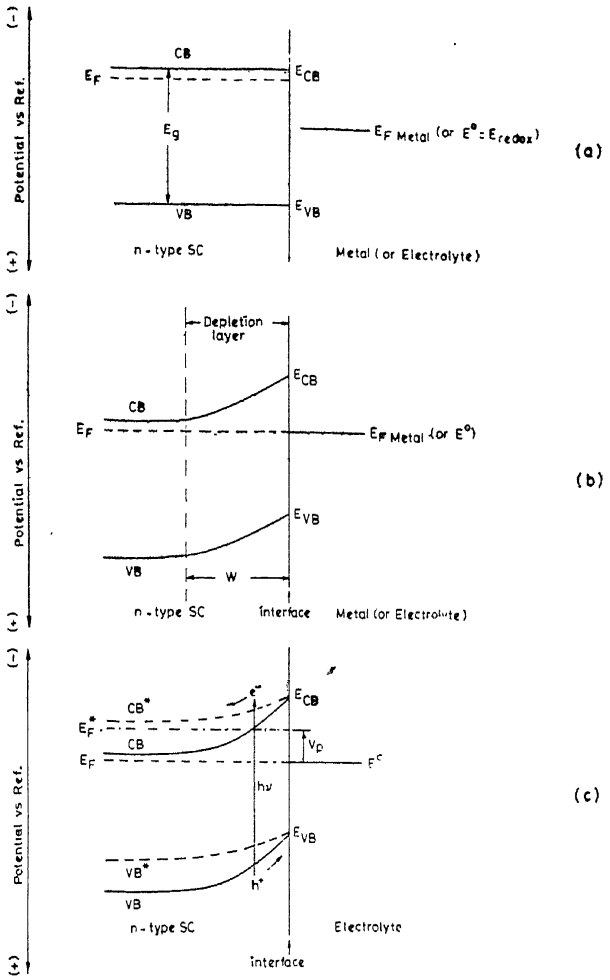

Figure 2. SC/electrolyte interface energetics ; **a.** *n*-type SC before contacting a metal or electrolyte (flat-band situation, $E_F = E_{fb}$). **b.** *n*-type SC in charge-transfer equilibrium with a metal (or electrolyte). **c.** *n*-type SC/electrolyte interface under illumination with $h\nu \geq E_g$. Asterisk indicates the steady state situation under illumination. Light generated holes move towards the surface whereas the electrons move towards the bulk of SC [E_{CB}, E_{VB}, the energies corresponding to the bottom of the conduction band and top of the valence band ; E_F and $E_{F,metal}$ Fermi levels of the SC and metal ; E^0 or E_{redox}, the standard electrochemical potential (= Fermi level) of the electrolyte ; E_g, the band gap of the SC ; W, the width of the depletion layer ; V_p, the photopotential].

most of this applied potential drops across the SC depletion layer. For a given SC the positions of the conduction and valence band edges, E_{CB} and E_{VB} respectively, at the surface, are considered to be fixed relative to a reference. The potentials are usually referred to a normal hydrogen electrode (NHE). (The Fermi level of NHE differs from the vacuum level by about 4·5 eV [40], *i.e.*, $E_{F,\ NHE} = -4{\cdot}5$eV (Lohman 1967). The Fermi levels of all the other redox systems can be given by $E_{F,Redox} = -(4{\cdot}5\ \text{eV} + eE^0)$). Under equilibrium conditions (figure 2b) $E_F = E^0$

and therefore, the bands are bent. The extent of band bending is measured as the barrier height E_B given by (1). An important reference potential namely 'flat-band potential' E_{fb}, is defined for a SC in contact with an electrolyte. This is the potential of the SC electrode measured relative to a reference electrode (such as NHE or SCE) when the SC bands are not bent and are flat right up to the surface. In other words, E_{fb} represents the position of the Fermi level of the SC when there is no band bending. Similar considerations are valid for *p*-type semiconductors as well (figure 3).

The Fermi level of the SC and hence the band bending can be varied by applying an external voltage or by optical excitation of the SC both of which modify the carrier distribution in the space charge region of the SC. Light of energy greater than the SC band gap (E_g) is absorbed and excess charge carriers are produced. The photogenerated electron-hole pairs in the space charge region are separated by the field existing therein. The majority carriers move towards the bulk and the minority carriers (electrons and holes respectively for *n*-type SC) towards the surface of the SC. The net effect is to produce a decrease of the potential barrier and the band bending. When the light intensity is sufficiently high the band bending is completely eliminated and flat-band condition is reached. Now, the electrochemical potentials of the two phases (SC and electrolyte) are no longer in equilibrium and tend to reach their original positions before contact. The difference in the Fermi levels of the two phases (and the band bending) can now be measured as the open circuit photopotential (V_p). Therefore, the maximum

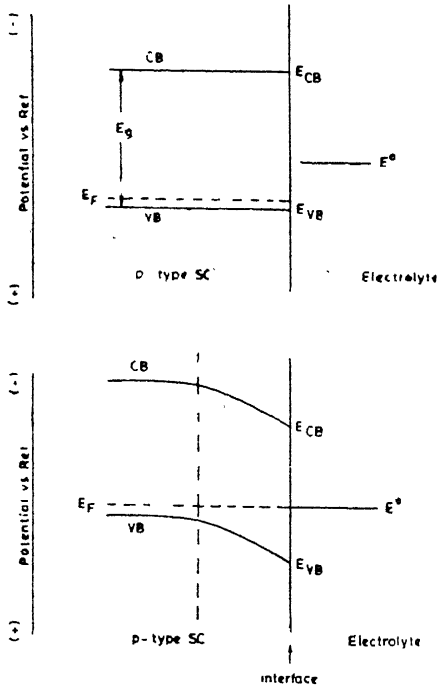

Figure 3. *p*-type SC/electrolyte interface energetics: a. SC before contacting the electrolyte. b. SC in charge-transfer equilibrium with the electrolyte.

value of photopotential obtainable for a given SC/electrolyte junction on illumination is given by

$$V_{P(\max)} = E_B = |(E_F - E^0)|. \quad (2)$$

From the point of view of energy conversion, it would be desirable to select redox couples whose E^0's lie very close to the E_{VB} for an *n*-type SC or E_{CB} for a *p*-type SC so that the ratio (E_B/E_g) is high. It is also implied in this model for SC/elctrolyte interface that only those redox systems having E^0's situated within the band gap of the SC can produce a useful SC/electrolyte liquid junction.

In the above discussion the effect of surface chemistry has not been taken into account. The surface of the SC has been assumed to be ' ideal ' in that there are no surface energy levels (surface states) present in the band gap, *i.e.*, a stateless band gap is assumed for the surface also. However, the real situation is far from ' ideal '. At the surface of a solid, the periodicity of the crystal is disrupted and the bonding forces are not saturated. Reorientation of the atoms at the surface and the unsaturated bonds create energy levels which lie in the band gap. These surface levels are called ' intrinsic ' surface states (Tamm levels) (Sze 1969). Also, ' extrinsic ' surface states can be produced by external factors such as adsorption, surface roughness etc. Several authors, especially Gerischer (1970), have taken into account the presence and their importance in the charge transfer processes. There have been several experimental observations by various workers suggesting the presence of surface states which facilitate electron transfer across the interface. According to Gerischer (1970), surface states are rather essential to observe currents across the interface. This is because according to the Franck-Condon principle, electron exchange is not possible between the electronic bands of the SC and the redox energy levels (which lie in the band gap) if the energy difference is more than $\pm kT$ (see figure 4). The diverse effects of such surface states on the energetics of the SC/electrolyte junction when they are present in very high densities lead to explanations based on various conceptual approaches, *e.g.*, Fermi level pinning (Bard *et al* 1980; Fan and Bard 1980 ; Bocarsly *et al*

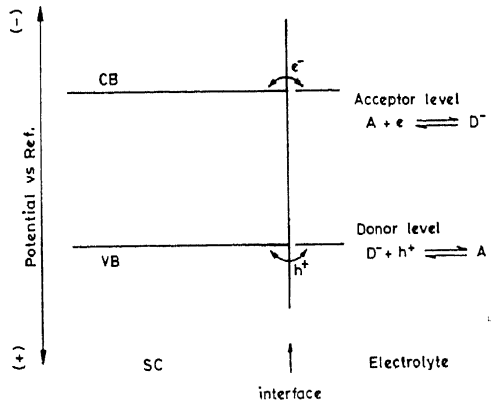

Figure 4. Location of energy levels for charge-transfer in the absence of surface states. For efficient charge-transfer the donor and acceptor levels should lie within ± kT (= 0·026 eV at 300 K) from the valence and conduction band edge energies (after Gerischer 1970).

1980 ; Schneemeyer and Wrighton 1980 ; Aruchamy and Wrighton 1980 ; Dominey *et al* 1981), inversion layer (Gobrecht *et al* 1978a ; Kautek and Gerischer 1980; Turner *et al* 1980), etc.

For many large band gap SC's experiments indicate that the positions of the SC energy bands at the surface (E_{CB} and E_{VB}) are independent of the doping density and the redox system in the electrolyte. However, when surface chemistry (of the dissociable surface groups) is influenced by the chemisorption of the solution species, the flat-band potentials are found to vary with the electrolyte composition. For oxides and several other SC's (*e.g.*, GaAs, Si, Ge) E_{fb} varies with the pH of the electrolyte at a rate of 59 mV/pH (Nernst equation) (Gerischer 1970). This is attributed to a dissociation equilibrium of surface hydroxide of the SC-controlled by the pH of the solution : *e.g.*, $Ge\text{–}OH + H_2O \leftrightharpoons GeO^- + H_3O^+$. In this surface reaction, an electronic charge is transferred from a place on the surface of the SC to a place in the outer Helmholtz layer of the electrolyte. This process is, therefore, controlled, at least partially, by the difference in the electrostatic potential between surface sites and the bulk of the electrolyte (ϕ_H). The thermodynamic considerations of this equilibrium process leads to a correlation,

$$\phi_H = \text{const} - \frac{2{\cdot}3\,kT}{q}\,[\text{pH}] - \log\,(f_{GeO^-} \cdot x_{GeO^-}), \tag{3}$$

where f_{GeO^-} and x_{GeO^-} are the activity coefficient and the mole fraction of GeO^- in the surface. As long as this mole fraction does not change to a larger extent by the variation in surface charges a linear relation between the flat-band potential (E_{fb}) and pH should be expected with a slope of 59 mV/pH. This relationship has been verified for a large number of semiconductors. Typical E_{fb} *vs* pH plots for $SrTiO_3$ and TiO_2 are given in figure 5. A similar influence of the anions in the electrolyte like S^{2-} and I^- has been found at semiconductors like Ge (Brattain and Body 1966; Body 1969), $MoSe_2$ (Gobrecht *et al* 1978b), etc. The effect of pH and anions in the electrolyte on E_{fb} of SC is different from Fermi level

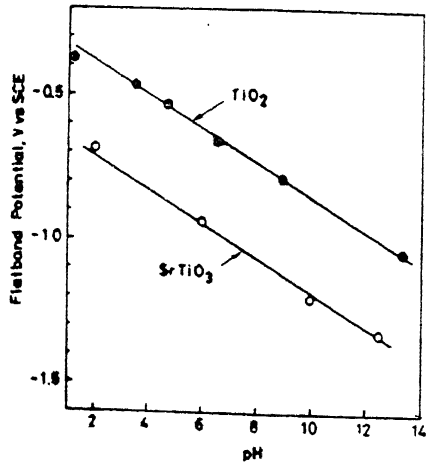

Figure 5. Variation of E_{fb} with pH of the electrolyte for *n*-$SrTiO_3$ and *n*-TiO_2 electrodes. From the slope, it follows that E_{fb} varies by 0·059 V/unit pH (after Watanabe *et al* 1976).

pinning (Bard *et al* 1980 ; Fan and Bard 1980 ; Bocarsly *et al* 1980 ; Schneemeyer and Wrighton 1980 ; Aruchamy and Wrighton 1980 ; Dominey *et al* 1981) and carrier inversion (Gobrecht *et al* 1978 ; Kautek and Gerischer 1980; Turner *et al* 1980) conditions since the latter are expected to arise due to intrinsic nature of the semiconductor surface and, therefore, are independent of the contacting metal or electrolyte.

The correlations between charge density and electrostatic potential have been derived for various conditions of the space charge layer. Since the electrostatic potential cannot be measured directly, the most valuable information has been obtained from capacitance measurements. The differential capacity C_{sc} for a fairly large band gap SC is given by the Mott–Schottky equation (Gerischer 1970)

$$\frac{1}{C_{sc}^2} = \frac{2}{\epsilon\epsilon_0 qN_D}\left(E - E_{fb} - \frac{kT}{q}\right). \tag{4}$$

Here, N_D is the concentration of donors (for n-type SC), ϵ and ϵ_0 are the dielectric constants of the vacuum and the SC, E is the electrode potential, E_{fb} is the flat-band potential of the SC, k is the Boltzman constant, T is the absolute temperature and q is the charge on the electron. This is a standard relationship used to determine the flat-band potential of a SC experimentally. Mott–Schottky plots for n-$SrTiO_3$, n-CdS and p-CdTe are given in figure 6.

2.2. *Current–potential relationships*

By considering a Schottky-type of barrier for a SC/electrolyte interface, current potential relationships can be derived. Schottky-barrier considerations are particularly valid when the reaction kinetics at the interface can be ignored. Reaction kinetics are generally described using the well-known Butler-Volmer equation

$$i = i_0 [\exp (\overleftarrow{\alpha} FE_a/RT] - \exp [-\overrightarrow{\alpha} FE_a/RT], \tag{5}$$

where i_0 is the exchange current density, E_a is the overpotential required to drive a current i through the electrode, F is Faraday constant and $\overleftarrow{\alpha}$ and $\overrightarrow{\alpha}$ are the transfer coefficients ($< 1{\cdot}0$). For $i \ll i_0$, the overpotential is negligible and the reaction kinetics does not limit the process. When $i \sim i_0$ reaction kinetics will become the rate limiting process. (The overpotential at the counter electrode can be minimized by having a large surface area). For a SC photoelectrode the charge transfer reaction is driven by the overpotential (Butler 1977)

$$E_a = E_g - E^0 - E_B, \tag{6}$$

where E_B is the band bending with the anode and cathode shorted together. For large band gap SC's E_a will be sufficiently large so that the reaction at the photoelectrode would not be rate limiting for light intensities of at least up to one sun ($\sim$100 mW/cm^2). Under these conditions, photoresponse of PEC's will be determined by the behaviour of photogenerated electron-hole pairs and thus the physical properties of the SC.

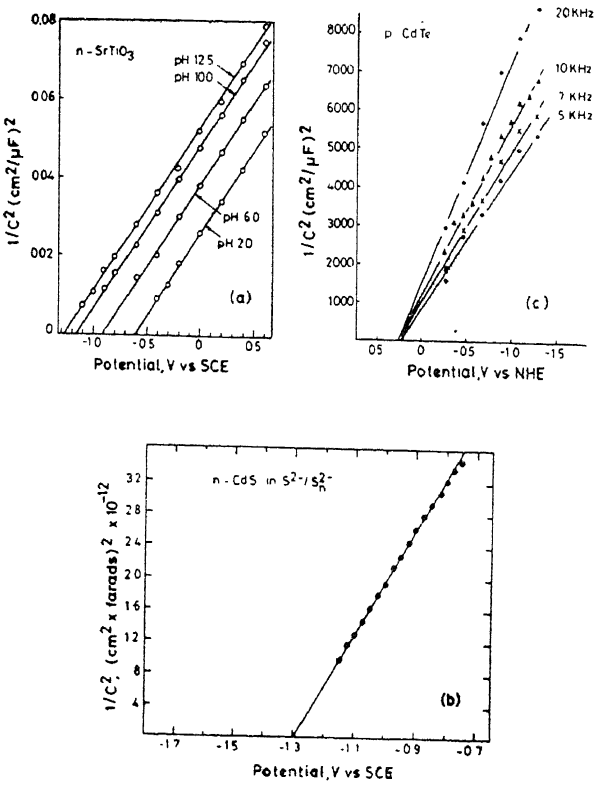

Figure 6. Plots of (differential capacitance)$^{-2}$ *vs* applied potential (at the SC electrode) (Mott–Schottky plots) for calculation of E_{fb} and N_d (carrier concn.). **a.** *n*-$SrTiO_3$ (aq. electrolytes at different pH values) (after Watanabe *et al* 1976). **b.** *n*-CdS in polysulfide electrolyte (after Ellis *et al* 1977). **c.** *p*-CdTe in 1 M NaOH (at various impressed ac frequencies) (after Ohashi *et al* 1977b).

The photocurrent flowing through the interface can be given by (Butler 1977.)

$$J = q\phi_0\left[1 - \frac{\exp\left[-\alpha W_0 (E - E_{fb})^{1/2}\right]}{1 + \alpha L_p}\right], \tag{7}$$

where ϕ_0 is the photon flux, α is the optical absorption constant, L_p is the hole diffusion length, q is the electronic charge and E is the electrode potential The depletion layer width W is given by

$$W = W_0 (E - E_{fb})^{1/2} = (2E/qN_D)^{1/2} (E - E_{fb})^{1/2} \tag{8}$$

where W_0 is the width of the depletion layer at a potential difference of one volt across it. This equation relates the photocurrent density with various parameters *viz.*, carrier density, diffusion length, flat-band potential, applied potential and optical absorption constant (α). The latter is given by

$$\alpha = \frac{A (h\nu - E_g)^{n/2}}{h\nu}, \tag{9}$$

where A is a constant, $h\nu$ is the photon energy and n depends on whether the electronic transition is direct ($n = 1$) or indirect ($n = 4$). Equations (7) and (8) help to describe the behaviour of the photocurrent in a Schottky junction. These equations also allow us to determine the nature of the fundamental optical transition and E_{fb} from the current-voltage characteristics.

2.3. *Light intensity dependence of photocurrent and potential*

Illumination of the SC/electrolyte junction with light of energy $h\nu \geqslant E_g$ gives rise to nonequilibrium situation in which the Fermi levels of the SC and redox electrolyte shift apart. Under open circuit conditions, the photopotential is a measure of the shift of Fermi levels (figure 2c). The maximum photopotential is given by (2). The variation of the photopotential with incident light intensity is given by an exponential relation, in analogy with a p–n junction (Memming 1978–79, 1980), *viz.*

$$V_P = \frac{kT}{q} \ln\left(1 + \frac{\triangle p}{p_0}\right) \approx \frac{kT}{q} \frac{\triangle p}{p_0} = \frac{kT}{q} \gamma I, \tag{10}$$

where p_0 is the density of holes in the bulk of the SC, $\triangle p$ is the increase in hole density on illumination, γ is proportionality factor and I is the light intensity. The photocurrent varies linearly with light intensity as in the case of p–n or SC/metal junction in solid state photovoltaics.

The factors which govern specifically the performance of photoelectrolysis cells and regenerative SC–liquid junction solar cells are discussed in the following sections.

3. Photoelectrochemical cells

3.1. *Photoelectrolysis cells*

In photoelectrolysis (also called photoassisted electrolysis) cells a net chemical reaction, such as the decomposition of water into H_2 and O_2, is driven by light energy absorbed by the SC. The free energy change ($\triangle G$) is positive and this energy is stored in the form of the photoelectrolysis products. For cells of this type the following energy balance can be written (Nozik 1976b, 1977b).

$$E_g - E_B - (E_{CB} - E_F) = \frac{\triangle G}{nF} + E_a^a + E_a + iR, \tag{11}$$

where E_{CB} is the conduction band energy and $\triangle G/nF$ is the free energy change per electron for the overall cell reaction. E_a^a and E_a^c are the respective overpotentials at the anode and cathode respectively and iR is the ohmic loss due to the internal resistance of the cell. The sum of the terms on the left side of (11) represents the net photon energy (as an electron–hole pair) available for doing the electrochemical work indicated by the terms on the right side of the equation. In the photoelectrolysis of water using n-type photoelectrode two redox reactions are involved (Tomkiewicz and Fay 1979), *viz.*

at anode (SC) : $H_2O + 2h^+ \rightarrow \frac{1}{2}O_2 + 2H^+$,

at cathode (Pt): $H^+ + e^- \rightarrow \frac{1}{2}H_2$.

Hence, the overall cell reaction is:

$$H_2O\,(l) \rightarrow H_2\,(g) + \tfrac{1}{2}O_2\,(g).$$

For this reaction, $\triangle H^0 = 68{\cdot}32$ k cals/mol (286 kJ/mol)

$$\triangle G^0 = 56{\cdot}69 \text{ k cals/mol (237 kJ/mol)}$$

$$\triangle H^0/nF = \frac{286 \times 10^3 \text{ J}}{2 \times 96\,500 \text{ C } (\equiv \text{J/V})} = 1{\cdot}48 \text{ V}$$

and $E^0 = \triangle G^0/nF = 1{\cdot}23$ V. Since $E^0_{H^+/H_2}$ (NHE) is zero (by definition, for the reaction $2H^+ + 2e^- \rightarrow H_2$), the decomposition potential of water can be taken as $E^D_{H_2O/O_2}$ (NHE) 1·23 V.

The energetics of the situation in the water photoelectrolysis cell is illustrated in figure 7. From the energy diagram it is possible to arrive at the properties of the SC photoelectrode for efficient photoelectrolysis of water without applying any external bias voltage. The conduction band should lie at a position more negative than the reversible hydrogen potential at a given pH. The band gap of the SC must be at least about 1·8 eV (Mavroides *et al* 1976: Mavroides 1978) (*i.e.*, 1·23 V + overvoltage) for the electrode reactions to take place. The overvoltages at the respective electrodes must be small. Above all these, an electrode satisfying the above criteria should be stable against photoanodic or chemical decomposition. The decomposition potential of the electrode should be more positive than the potential of the H_2O/O_2 redox level. However, in most cases where the energetics is appropriate, kinetic processes control the overall efficiency of the photoelectrolysis cell. For many SC's the disposition of the energy bands (E_{VB} and E_{CB}) in relation to the redox levels of the aqueous electrolyte is not conducive for photoelectrolysis without an applied bias voltage. For example, in the case of TiO_2 ($E_g = 3{\cdot}01$ eV) electrode the position of the conduction band lies at a more positive potential than the hydrogen evolution potential. It requires an additional bias (0·2–0·5 V) for hydrogen evolution to take place (Wrighton *et al* 1976; Mavroides *et al* 1975, 1976; Mavroides 1978).

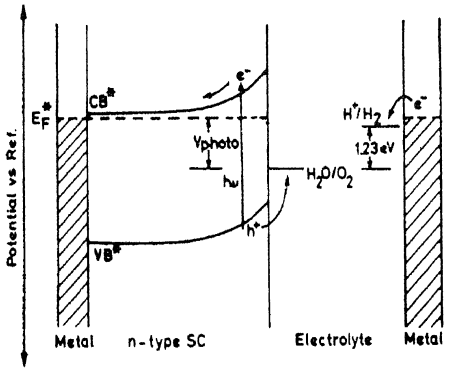

Figure 7. Energetics for a water photoelectrolysis cell employing an *n*-type SC. Asterisk indicates steady state situation under illumination. V_{photo} is the open-circuit photopotential of the cell. At anode: $H_2O + h^+ \rightarrow \frac{1}{2}\,O_2 + H^+$; at cathode: $H^+ + e^- \rightarrow \frac{1}{2}\,H_2$.

This is because, the electrons arriving at the metal counter electrode, without applied bias, are not energetic enough to reduce the H^+ ions. With $SrTiO_3$ ($E_g = 3{\cdot}2$ eV), however, the energetics is favourable and photoelectrolytic decomposition of water without any applied bias (at a pH 13) has been noticed (Wrighton *et al* 1976 ; Mavroides *et al* 1976 ; Mavroides 1978).

Butler and Ginley (1978) have attempted to relate the fundamental properties of the SC's to the measurable quantities, such as the flat-band potential, in order to evolve a systematic approach for the design and development of materials for water photoelectrolysis cells. They relate the electron affinity E_e to the flat-band potential (E_{fb}) by

$$E_e = E_R - E_{FC} + q\,(E_{fb} + E_c) \tag{12}$$

where E_R is the difference between the vacuum level and the reference electrode level (4·5 eV for NHE), E_{FC} is the difference between the Fermi level and the bottom of the conduction band (E_{CB}), and E_c is the correction to the flat-band potential due to adsorption of charges on the surface of the SC. These considerations show that for optimum efficiency at short circuit conditions for photoelectrolysis the semiconductor should have as small an electron affinity as possible (5·3 eV). E_e can be calculated from the individual electronegativities (χ_A and χ_B) of the constituent atoms of a binary compound AB_2 possessing a band gap (E_g) by (Butler and Ginley 1978)

$$E_e = (\chi_A \chi_B^2)^{1/3} - (E_g/2). \tag{13}$$

For enhanced efficiencies of photoelectrolysis, *p–n* type cells in which both the electrodes (*n*-and *p*-type SC's forming the cell) are simultaneously illuminated have been examined by various workers (Nozik 1976a, 1977a ; Ohashi *et al* 1977a ; Bockris and Uosaki 1977 a; Jarrett *et al* 1980a). A major difference between a Schottky type and *p–n* type photoelectrolysis cells is that a one-photon process is operating in the former, while in the latter a two-photon process is involved. For this kind of heterotype *p–n* cell, the two-photon process leads to energy upconversion in that the net potential energy available for doing chemical work is greater than the energy represented by one photon.

3.2. *Semiconductor/electrolyte junction (regenerative) solar cells*

A photoelectrochemical cell can be used to produce electricity by choosing redox systems such that the reactions taking place at one of the electrodes is completely reversible at the counter electrode. In this situation no net chemical reaction occurs and $\triangle G = 0$. This mode of operation is called photovoltaic or regenerative solar cell mode. The energetics for a regenerative cell is given in figure 8. The nature of photoeffect is identical to that in the photoelectrolysis cell. The materials problems, however, appear somewhat less stringent in these cells than in photoelectrolysis cells. A wide variety of redox couples can be chosen to give maximum light to-electricity conversion. The processes occurring at the electrodes are, at the anode : Red + $h^+ \rightarrow$ Ox ; at the cathode: Ox + $e^- \rightarrow$Red. The redox system is not thus consumed in the over all cell reaction. The maximum value of energy conversion efficiency that can be obtained with a SC/redox system is severely reduced by corrosion problems which limit the

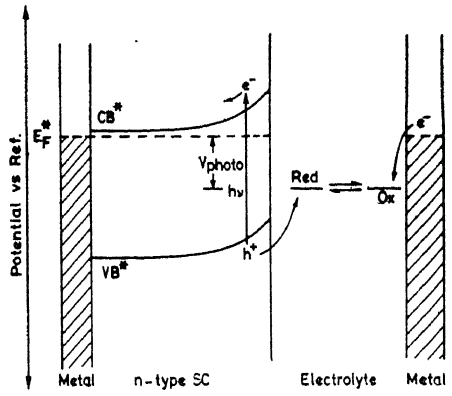

Figure 8. Energetics for an *n*-type SC/electrolyte junction (regenerative) solar cell. Asterisk indicates the steady state situation under illumination. V_{photo} is the open-circuit photopotential of the cell. At anode : $Red + h^+ \rightarrow OX$; at cathode : $OX + e^- \rightarrow Red$.

selection of redox couples. These difficulties are discussed in a subsequent section.

4. Efficiency considerations

The photovoltaic devices are threshold devices (*i.e.*, quantum converters). The energy conversion efficiency (η) of any threshold device is given by (Gerischer 1977b)

$$\eta = \frac{E_{stor} \int_{E_{th}}^{\infty} A(E)N(E)dE}{\int_{0}^{\infty} EN(E)dE}. \tag{14}$$

η can be simply defined as the ratio of the output electrical or chemical power from the cell to the total optical energy input. The threshold energy E_{th} is the optical energy (band) gap of the SC and the stored energy E_{stor} is the cell voltage. $A(E)$ characterizes the absorbance of the SC and $N(E)$ is the flux density of incident photons. Since the solar spectrum extends over a wide energy range, only a limited amount of free energy can be converted and used for work in the solar energy conversion *via* PEC's because of restrictions on the values of E_g. For photovoltaic SC devices the free energy conversion efficiency depends on the band gap and reaches maximum for $E_g \sim 1{\cdot}2$–$1{\cdot}5$ eV (Fischer 1974; Ehrenreich and Martin 1979). For the photoelectrolysis cells which produce chemicals (*e.g.*, H_2 from water) with an applied bias, solar energy conversion efficiency is given by

$$\eta = \frac{[(\text{energy stored as fuel}) - (\text{electrical energy supplied})]}{(\text{incident solar energy})}. \tag{15}$$

Energy stored in the fuel is released when the fuel is suitably burnt (oxidized). The optical to electrical energy conversion efficiency in a SC/liquid junction solar cell is given by

$$\eta = \frac{(I \times V)_{max}}{P} \times 100 \tag{16}$$

where $(I \times V)_{max}$ is the maximum output power of the solar cell and P is the light (optical power) input. In addition to η, a parameter namely fill factor (FF) is defined in a PEC :

$$FF = \frac{(I \times V)_{max}}{I_{sc} \times V_{oc}} \tag{17}$$

where I_{sc} is the short circuit photocurrent and V_{oc} is the open circuit photovoltage. The fill factor (<1) indicates the extent of departure from the ideal behaviour of the SC/electrolyte junction.

The theoretically attainable upper limits of solar energy conversion efficiencies in PEC's have been estimated by various workers. According to Gerischer (1977b) for single electrode based PEC's employing SC's having band gaps 1·2–1·5 eV, the maximum η for operation in the regenerative (light to electricity) mode is 25–30% and for water photoelectrolysis 20–30% (see table 1). Mavroides and co-workers (Mavroides 1976 ; Mavroides 1978) considering 1·8 eV as the optimum band gap for photoelectrolysis estimate the maximum η as 25%. For double photoelectrode based (p–n) water photoelectrolysis cells a maximum η value of 45% is given by Nozik (1976a, 1977a) Anon (1979). As will be seen later, solar-to-electricity conversion efficiencies as high as 12–14% have been achieved in n-GaAs (surface treated with Ru^{3+}) and n-WSe_2 (tables 1 and 5) based PEC's. A 12% efficient photoelectrolysis cell (solar-to-hydrogen) has been announced recently by Heller and Vadimsky (1981) in which a specially surface-treated p-InP serves as the photocathode. It is gratifying to note that the above values represent 50% of the theoretically attainable limits of η.

In addition to these overall energy conversion efficiencies two other efficiency criteria are referred to in PEC's. They are current efficiency and quantum efficiency.

$$\text{Current efficiency} = \frac{\text{Actual no. of moles of substance produced}}{\text{No. of moles of substance expected for the actual current flow}} \tag{18}$$

For example, one ampere of current flow should electrolyse water to produce 5·2 micromoles of H_2 and 2·6 micromoles of O_2 per sec (Faraday's second law). The current efficiencies for H_2 and O_2 production are found by dividing the actual quantities of gases formed by the theoretically expected values for an ideal process. This is true provided no other products are formed, *e.g.*, H_2O_2, along with O_2 at the anode. The quantum efficiency ϕ_e is the ratio between the number of electrons which flow in the external circuit under short circuit to the number of photons which strike the photoelectrode surface. Usually quantum efficiencies are calculated by applying external bias high enough to saturate the photocurrent. ϕ_e should be close to unity in the ideal case.

5. Photocorrosion and stability of semiconductor photoelectrodes

Most SC's which otherwise satisfy the energetic requirements for use in PEC's are found to be susceptible to photocorrosion reactions. This serious difficulty excludes several visible light responding, non-oxidic SC's as photoelectrodes in photoelectrolysis cells. The decomposition reactions are electrochemical reactions and they are associated with an electrochemical potential represented by E_D^0 (Gerischer 1977a ; Bard and Wrighton 1977), the decomposition potential. Most SC's have their E_D^0's lying in the band gap of the SC on the energy scale. This would mean that for *n*-type SC's the holes at the valence band edge are energetically capable of oxidizing the SC in addition to oxidizing a redox couple lying in the band gap (figure 9). It is, therefore, expected to find photocorrosion in these cells. However, the stability of the electrode depends on the rate of charge-transfer to the redox levels in the electrolyte (Wrighton 1979). For an *n*-type SC, if the rate of hole transfer to the solution species is very high compared to that to SC which leads to the decomposition process, the electrode will experience minimum degradation and will be stable over a considerably longer period of time. It is found for *n*-type SC's that the redox couples should lie negative of the decomposition potential to give electrode stability (Bard and Wrighton 1977). The decomposition reaction limits the maximum efficiency obtainable because the maximum band bending possible would only be $|E_F - E_D^0|$. If the redox couple chosen has an E^0 more negative than the E_D^0, the band bending will be much less ($|E_F - E^0|$). In the case of *p*-type SC's dark anodic decomposition reactions are expected due to the presence of excess holes at potentials positive of E_{t_b} (Bard and Wrighton 1977). Cathodic decomposition reactions are also possible for *p*-type SC's. Usually, decomposition reactions involve

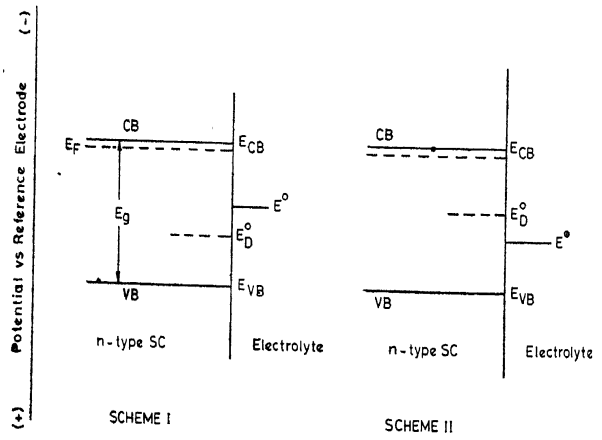

Figure 9. Interface energetics for *n*-type SC/electrolyte junction, taking into account of the decomposition potential, E_D^0, of the SC. Scheme I : Situation for E_{redox} ($= E^0$) more negative than E_D^0. In this case, the primary oxidation product, 'OX' (from the reaction Red $+ h^+ \rightarrow$ OX) is not capable (thermodynamically) of oxidizing the SC. If 'Red' can successfully capture 100% of the photogenerated holes, SC will be completely stable to photoanodic dissolution. Scheme II. E_{redox} is more positive than E_D^0. Oxidized form of the redox couple, 'OX' (with a redox potential E_{redox}), is capable (thermodynamically) of spontaneously oxidizing the SC in dark.

several steps and hence they are kinetically slow. When simple reversible redox couples with suitable E^0's are chosen the electrode may be stabilized. Considerable success has been found in SC/liquid junction solar cells in stabilizing the photoelectrodes by choosing the redox system based on these considerations. It appears that, in many systems exhibiting good stability, the redox electrolyte specifically interacts with the surface of the SC electrode.

Surface modification techniques like the deposition of a suitable oxide or a metal over the low band gap SC (Bockris and Uosaki 1976; Nakato *et al* 1976 ; Morisaki *et al* 1976 ; Tomkiewicz and Woodall 1977 ; Gourgaud and Elliott 1977 ; Kohl *et al* 1977), a surface derivatization with redox species (Wrighton *et al* 1980) have also been attempted with limited success for stabilizing the SC photoelectrodes. Studies by Heller and co-workers (Parkinson *et al* 1978a,b ; Heller *et al* 1981; Heller and Vadimsky 1981; Johnston *et al* 1980 ; Heller 1980) have indicated that surface modification of the SC by strong chemisorption of metal ions or oxygen alters the role of surface states and reduce surface recombination losses leading to improved efficiency and stability of the PEC. Nonaqueous electrolytes have also been studied in PEC's and found to impart better stability in some cases to photoelectrodes than the aqueous electrolytes (Bard and Kohl 1977).

6. Semiconductor electrode characteristics for PEC's

Most of the requirements for an efficient solid state (p–n) solar cell are equally desirable for SC's used in PEC's (Loferski 1956 ; Hovel 1975 ; Bard 1979). Additionally, the electrode materials must be stable against photocorrosion and dark chemical attack (Gerischer 1977a; Wrighton 1979; Bard 1979). Desired solid state properties of SC's are : $E_g \sim 1{\cdot}2$–$1{\cdot}5$ eV, and direct band gap ; high α ; long minority carrier life-time (τ) and high carrier mobility (μ), $\mu \times \tau \sim 10^{-8}$ cm^2/V ; good electrical conductivity ($R \sim 0{\cdot}01$–10 Ω-cm) ; carrier concentration $\sim 10^{16-19}$/cm^3. For photoelectrolysis cells, however, the requirements are more stringent if the desired reaction is the water photoelectrolysis. The minimum energy gap of the semiconductor should be $1{\cdot}23$ eV, the decomposition potential of water. Due to overvoltages at the electrodes and the effect of surface states on the interface energetics a much higher value for the band gap ($1{\cdot}8$–$2{\cdot}5$ eV) of the SC is required. The flat-band potential of the n-type SC should be more negative than $-0{\cdot}83$ V *vs* NHE at pH $\simeq$ 14 for photoelectrolysis without external bias (Bockris and Uosaki 1977b). (This requires that the electron affinity of the SC should be less than $5{\cdot}3$ eV). Such ideal SC's have not yet been realized for maximum possible solar energy conversion.

7. Experimental methods of investigation of photoelectrochemical processes

Semiconductor/electrolyte interfacial processes can be studied by various electrochemical experimental techniques which are usually employed in the study of metal/electrolyte junctions. Current-voltage (i-v) characteristics, capacitance behaviour and the power characteristics are the most essential studies made on

these systems. Current-voltage characteristics in dark and under illumination of the SC/electrolyte junction provide information concerning the electrochemical reactions taking place, nature of the junction and the semiconductor band energies including E_{fb}. Current flowing across the junction (or interface) is monitored as a function of applied voltage in the dark and under illumination. Usually potentiostatic *i-v* measurements are made using a standard 3-electrode geometry. The semiconductor is the working electrode, and an inert electrode (Pt or C) functions as a counter electrode. A suitable reference electrode (*e.g.*, SCE, Ag/AgCl, etc.) is used to refer the potential applied to the SC working electrode. Steady state (or equilibrium) as well as fast potential scan current-potential measurements are very useful. Typical steady state *i-v* curves for *n*-$SrTiO_3$ and *n*-CdS are represented in figure 10. Cyclic voltammetry, a fast potential scan method, has been extensively used in recent years to examine surface processes of semiconductors in PEC's such as the probing of surface state effects, redox reactions of surface confined species at SC, surface passivation, etc. (For a schematic of an *i-v* measurement set-up, see figure 1b). In the study of electrode

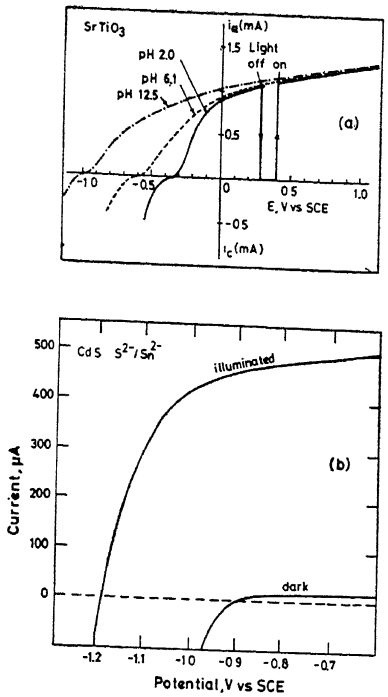

Figure 10. Typical current-voltage (*i–v*) characteristics of (a) *n*-$SrTiO_3$ single crystal electrode under (anodic polarization) illumination ($h\nu \geqslant 3{\cdot}2$ eV). Dependence of photocurrent onset potential with pH is also shown (after Watanabe *et al* 1976); (b) *n*-CdS single crystal electrode in 1 M Na_2S–1 M S–1 M NaOH (after Ellis *et al* 1976). The potential of photocurrent onset, E_{onset}, can be taken as the flat-band potential, E_{fb}, at sufficiently high light intensities. The saturation of photocurrent (potential independent behaviour) is due to the light intensity limited minority carrier generation. Efficient electron-hole pair separation in the space charge layer and charge transfer across the interface are characterized by a steep rise in photocurrent and a high saturation value.

stability the rates of the competitive reactions, *viz.*, the photodecomposition and the desired charge-transfer process to a solution species will determine the extent to which the corrosion reaction will be suppressed by a solution redox system. Rotating disc electrode (RDE) and rotating ring disc electrode (RRDE) methodologies have been applied in certain recent studies for the evaluation of the capability of various redox systems in suppressing the photocorrosion reactions (Inoue *et al* 1977 ; Miller *et al* 1977b). The disc electrode is the SC crystal and the ring electrode is a suitable inert electrode (Pt, Au, etc). An example of a study of competitive oxidation of redox species by RRDE technique at *n*-CdS electrode is given in figure 11.

Capacitance-voltage measurements are used in the determination of the flat-band potential. The Mott–Schottky relationship (equation (4)) which relates the

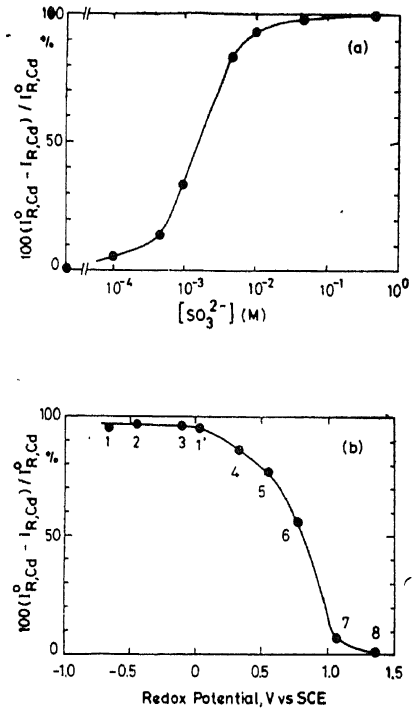

Figure 11. Percentage dissolution (photocorrosion) suppression of CdS electrode determined by rotating ring disc electrode techniques (disc : CdS single crystal ; ring : amalgamated Cu ring). (a) Percentage of dissolution suppression as a function of aq SO_3^{2-} concentration (dissolution reaction: $CdS + 2h^+ \rightarrow Cd^{2+} + S$). (b) Percentage of dissolution suppression by reducing agents (conc. for all 0·01 M) as a function of their redox potential

1. SO_3^{2-}/SO_4^{2-} ; 1′. $SO_3^{2-}/S_2O_6^{2-}$; 2. S^{2-}/ S; 3. $S_2O_3^{2-}/S_4O_6^{2-}$; 4. $Fe(CN)_6^{3-/4-}$; 5. I^-/I_2 ; 6. $Fe^{2+/3+}$; 7. Br^-/Br_2 ; 8. Cl^-/Cl_2.

$I_{R,cd}$, the limiting current at the ring electrode corresponding to the reduction of Cd^{2+} for the electrolytes containing a reducing agent. $I^0_{R,cd}$ for that without the reducing agent added. As can be seen, 1, 2, 3, and 1′, give ~ 100% corrosion suppression (after Inoue *et al* 1977).

electrode potential with the interfacial capacitance is used to obtain E_{fb} from capacitance data (figure 6). These measurements as a function of excitation frequency ($10^1 - 10^6$ Hz), in many cases, give valuable information about the effect of surface states (Memming 1964 ; Dutoit *et al* 1975). Normally a semiconductor surface, free of surface states, would give frequency-independent capacitance values and a constant E_{fb}. When the surface states are present to a considerable extent, the capacitance and E_{fb} values vary with excitation frequency. In certain cases, measurement of photocapacitances (*i.e.*, capacitance of the illuminated SC electrode) also helps in the study of surface energy levels (Mavroides 1977).

Performance evaluation of the PEC's consists of determination of various cell parameters. As mentioned earlier (§§ 1–4) various efficiencies are determined for a PEC. Quantum efficiency (ϕ_e) of a cell relates to the characteristics of a depletion layer such as depletion layer thickness, diffusion length and recombination of the charge carriers, provided the kinetics of interfacial processes is not rate-limiting. Usually monochromatic quantum efficiencies are measured under an applied bias such that the photocurrent lies in the saturation region, where the current is limited only by the monochromatic light intensity (minority carrier generation rate). Quantum efficiencies vary as a function of wavelength at energies greater than the band gap energy. Measurement of quantum efficiencies can be used to evaluate the nature of the optical transition in the SC (allowed or direct and indirect or forbidden transitions). The wavelength response of the photoelectrochemical cell can be given by the following equation [see, (7)–(9)] (Butler 1977) :

$$(\phi_e h\nu) = (L_p + W_0(E - E_{fb})^{1/2})\ A\,(h\nu - E_g)^{n/2} \qquad (19)$$

where ϕ_e is the quantum efficiency. A plot of ln $(\phi_e h\nu)$ *vs* ln $(h\nu - E_g)$ will be a straight line with a slope of $n/2$. It has been found that the direct band gap materials are better suited for solar energy conversion devices.

Illumination of the SC electrode is performed by various methods. Quantum efficiency, monochromatic energy, conversion efficiency and spectral response are measured using either a laser or monochromatized light. For solar conversion measurements in the laboratory usually a high pressure Xe-lamp (solar simulator) whose spectral output is similar to that of the solar spectrum (AM2) is used. Many a time, cell parameters measured under direct sunlight are reported.

Study of the surface processes has been an interesting area very much pursued in recent years. Luminescence studies at the SC surfaces in contact with electrolytes have been used in locating the position and the density of extrinsic surface states or impurity (or defect) states (Mavroides 1977 ; Ellis and Karas 1979, 1980). Sub-band gap photoresponse measurements have also been found to give important information regarding the surface energy levels (Morisaki *et al* 1976 ; Mavroides and Kolesar 1978 ; Laser and Gottesfeld 1979 ; Butler *et al* 1981). In addition to the above techniques, microscopic and spectroscopic techniques such as SEM, XPS, Auger, etc., have been used successfully in recent years in the characterization of SC surfaces (Kohl *et al* 1977 ; Harris and Wilson 1976 ; Harris *et al* 1977; Lawerenz *et al* 1980; Cahen *et al* 1978; Sayers and Armstrong 1978 ; Noufi *et al* 1979 ; Heller *et al* 1978).

8. Semiconductor electrode materials

Semiconductors have been used in single crystal as well as in polycrystalline forms. In general, measurements on single crystals are reproducible and reliable. Measurements on polycrystalline materials are influenced by the grain size, grain boundary recombination, intergrain resistance, etc. Single crystals can be obtained from commercial sources with the desired dopant concentration, conductivity, orientation, purity, etc. They are made by standard crystal growing methods (melt growth, vapour transport, epitaxy, flame fusion, etc.). Preparative methods of polycrystalline materials, however, are diverse and photovoltaic properties can be significantly different from those of single crystals. Polycrystalline thin film electrodes, reported in the literature, are prepared by one of the following methods : chemical vapour deposition (CVD), spray pyrolysis, electrochemical deposition, or vacuum evaporation. In case of certain binary oxide and chalcogenide semiconductors, thin layers of the compounds are formed over the basic metal itself by thermal or electrochemical method (*e.g.* TiO_2, Nb_2O_5, WO_3, SnO_2, CdS, CdSe, Bi_2S_3). Pressed and sintered compacts of SC powders also have been used. Pressure sintering (or hot pressing) of powders yield high density samples and give rise to good photoeffects. Polycrystalline materials are economical to single crystals and in PEC's polycrystalline thin film electrodes are found to perform extremely well. Mixed SC's such as $CdSSe_{1-x}$ (Kohl and Bard 1978), $CdSe_xTe_{1-x}$ (Hodes 1980) also have been studied. Interestingly n-$CdSe_{0.65}$ $Te_{0.35}$ has been found to be stable in PEC containing polysulfide electrolyte yielding a solar light-to-electricity conversion efficiency of $\sim$8% whereas n-CdTe is not stable in the same electrolyte. Increased efficiencies have been reported with special electrodes such as n^+n-GaAs (Noufi *et al* 1980) and n-GaAs/n-CdS (Wagner and Shay 1977). Other requirements of physical characteristics such as electrical conductivity, carrier mobility, diffusion length, etc., are optimized as for solid state solar cells. The surface of the electrode has to be prepared by suitable etching treatment to obtain good conversion efficiencies. Etching produces a new surface by removing the damaged surface layer of the crystal and impurities on the surface. Preferential etching of certain planes of the SC leads to a ' textured surface ' (matte or hillock) which minimizes the light reflection losses and increases the area for reaction. It is equally important for polycrystalline materials also. Etch treatments are different for different electrodes and there appears to be no standard etchants suitable for all the SC's. (e.g., CdS can be etched in conc. HCl ; CdSe is etched using a mixture of conc. HNO_3 and HCl in the ratio 4 : 1 followed by a treatment in 10% KCN ; GaAs is etched in a 1 : 1 solution of 30% H_2O_2 and H_2SO_4 ; CdTe can be etched in 5% Br_2-methanol solution). Also, selection of etchant depends on the desired surface morphology. Controlled etching can also be done by ' photoetching ' of the SC in a PEC in which the SC undergoes photocorrosion during illumination with the removal of surface material. Back contact to a lead wire has to be made ohmic by a suitable metal alloy contact.

9. Survey of important semiconductor electrodes studied in PEC's

9.1. *Photoelectrolysis cells*

A large number of simple and mixed oxides have been examined for photoeffect and possible utilization as photoelectrodes for the decomposition of water employing solar or simulated light. Most of the oxides are *n*-type SC's. Only large band gap (~3·0 eV) oxides have been found to be stable to photocorrosion and have suitable photoelectrochemical characteristics. Low band gap oxides usually have either more positive flat-band potentials or poor space charge characteristics. TiO_2 ($E_g = 3{\cdot}01$ eV) and $SrTiO_3$ ($E_g = 3{\cdot}2$ eV) have been studied very extensively in photoelectrolysis cells. $SrTiO_3$ has been the only oxide till now to give high quantum and optical-to-chemical conversion efficiencies (see table 3). It does not require any external bias voltage for effecting photoelectrolytic decomposition of water. However, $SrTiO_3$ is of less practical value due to its large E_g. A few *p*-type oxides such as CuO (Hardee and Bard 1977) have also been examined in PEC's. A recent report (Jarrett *et al* 1980) of a *p–n* photoelectrolysis cell containing *p*-$LuRhO_3$ and *n*-TiO_2 photoelectrodes is interesting. $LuRhO_3$ is a low band gap (2·2 eV) SC and exhibits good photoeffect and stability. In the above cell, photoelectrolysis was found to take place without any externally applied bias voltage and with the visible light illumination of the photocathode, *i.e.*, $LuRhO_3$. The efficiency of solar-to-optical conversion was, however, $< 1\%$. There have been several attempts made to sensitize the large band gap SC's to visible light. Doping with transition metal ions like Cr^{3+} was found to give visible light-induced photocurrents in certain oxides (Ghosh and Maruska 1977 ; Wrighton *et al* 1975 ; Houlihan *et al* 1978). Dye sensitization of SC's (Goodenough *et al* 1980 ; Gerischer and Willig 1976 ; Tsubomura *et al* 1976 ; Matsumura *et al* 1977 ; Watanabe *et al* 1980 ; Yamase *et al* 1979 ; Clark and Sutin 1977 ; Memming *et al* 1979 ; Memming and Schroppel 1979 ; Campet *et al* 1980 ; Hamnet *et al* 1980 ; Alonso *et al* 1981) has also been studied in which dye molecules attached to the SC surface absorb the visible light and transfer the charges to the SC. These methods have met with only limited success in improving the light-to-chemical energy conversion efficiencies. Certain *p–n* photoelectrolysis cells (Yoneyama *et al* 1975 ; Nozik 1976, 1977 ; Ohashi *et al* 1977a ; Jarrett *et al* 1980) (table 4) have been investigated with the aim of coupling the energy of two photons to effect photoelectrolysis of water without an external bias voltage. As can be seen from table 4 most *p–n* combinations studied suffer the disadvantage of poor matching of their energetics. Literature data on various oxide photoelectrodes are summarised in table 3.

A few low band gap, non-oxidic SC's including the layer-type compounds like MoS_2, $MoSe_2$ have been studied in photoelectrolysis cells (Nozik 1976a 1977a; Ohashi *et al* 1977a,b; Heller *et al* 1981; Bockris and Uosaki 1976, 1977a; Tributsch 1977; Bookbinder *et al* 1979). Most non-oxidic SC's, however, are not stable in such cells. *p*-type electrodes like *p*-Si, *p*-GaP and *p*-InP can serve as photocathodes but have very high over potentials for hydrogen evolution reaction (Nakato *et al* 1976 ; Bookbinder *et al* 1979 ; Dominey *et al* 1981). In order to improve the kinetics of H_2-evolution, surface modification of the photocathodes

Table 3. Data on various semiconducting oxides (SC) studied in PEC's[a]

SC electrode[b] (EA, eV ; χ)	E_g, eV[c] (λ_{onset}, nm)	E_{fb},[d] V *vs* SCE (pH = 13)	η[e]	Remarks[f]	Ref.
(1)	(2)	(3)	(4)	(5)	(6)
TiO_2 (4·33 ; 5·83)	3·01 (415)	—1·1	1–2% (351, 364 nm laser illum. V_{appl}, 0·5 V)	Xtal ; stable ; $\phi_e = 10$–20% for $\lambda = 351$, 364 nm ($\phi_e = 1{\cdot}2\%$ without applied bias)	Wrighton *et al* (1975)
			0·4% (sunlight ; bias applied by pH gradient of ~ 13)	TiO_2 prepared by thermal oxidation of Ti over bunsen flame (pc)	Fujishima and Honda (1975)
			0·7% (sunlight ; bias applied)	Boron doped Ti sample oxidized in natural gas flame (pc)	Houlihan *et al* (1979)
			1·3% (sunlight)	Al-doped Xtal TiO_2	Ghosh and Maruska (1977)
$SrTiO_3^g$ (3·71 ; 5·27)	3·2 (400)	—1·3	20% (330 nm ; V_{appl}, 0·25–0·4 V)	Xtal ; stable ; $\phi_e = 100\%$ for $\lambda \leqslant 330$ nm ($V_{appl} \geqslant 1{\cdot}5$ V)	Wrighton *et al* (1976)
$BaTiO_3$ (3·6 ; 5·19)	3·3–3·4 (376)	—1·22	...	Xtal ; stable ; $\phi_e = 30\%$ (V_{appl}, 4V ; 360 nm)	Quinn *et al* (1976)
Fe_2O_3 (4·71 ; 5·88)	2·2	—0·67	...	Xtal ; stable ; $\phi_e = 20\%$ (V_{appl}, 0·5 V ; 365 nm)	Butler *et al* (1976)
SnO_2 (4·49 ; 6·24)	3·5 (350)	—0·82	...	Xtal ; stable ; $\phi_e = 27\%$ (254 nm)	Wrighton *et al* (1976)

Table 3—*Contd.*

(1)	(2)	(3)	(4)	(5)	(6)
WO_3	2·8	—0·20	...	Xtal ; stable ; $\phi_e = 70\%$ (275–310 nm)	Buttler *et al* (1976)
ZrO_2 (3·42 ; 5·92)	5·0	—2·04[h]	...	stable (oxide film on Zr)	Clechet *et al* (1976)
Ta_2O_5 (4·08 ; 6·38)	4·0	—1·44[h] —1·20[h]	... ...	stable (oxide film on Ta)	Clechet *et al* (1976) ; Aruchamy *et al* (unpublished)
Nb_2O_5	3·4	—1·22[h] —1·10[h]	...	stable (oxide film on Nb)	do.
CdO	2·1	—0·20	...	pc ; unstable	(Kung *et al* 1977)
V_2O_5	2·75	+0·45	...	pc ; unstable ; poor photoresponse	Hardee and Bard (1977)
ZnO (4·15 ; 5·75)	3.2	—1·00	...	Xtal ; unstable	Gerischer (1977)
Sb_2O_5	3·0	—0·74	...	pc ; —	Metikos-Hukovic and Lovrecek (1978)
Bi_2O_3	2·8	—0·32	...	pc ; unstable	Hardee and Bard (1977)
PbO	2·8	—0·54	...	pc ; unstable	do.
p-CuO	1·7	+0·06	...	pc ; unstable	do.
$FeTiO_3$ (4.3 ; 5.72)	2·16	+0·10	...	Xtal ; unstable ; $\phi_e = 15\%$ (350 nm)	Ginley and Butler (1977)

$FeTiO_3$ (ordered)	2·58	—0·60	...	Xtal ; —	Ginley and Butler (1977)
Fe_2TiO_5	2·18	+0·50	...	Xtal ; $\phi_e = 15\%$ (350 nm)	do.
$YFeO_3$	2·60	—0·46	...	Xtal ; stable	Butler *et al* (1977)
$CaTiO_3$	3·40 (400)	—1·13[h]	...	pc ; stable	Kung *et al* (1977)
$Hg_2Ta_2O_7$	1·80 (650)	+0·20[h]	...	pc ; unstable	do.
$Hg_2Nb_2O_7$	1·80 (650)	+0·30[h]	...	pc ; unstable	do.
$PbFe_{12}O_{19}$	2·30 (550)	+0·20[h]	...	Xtal ; stable	do.
$PbTi_{1·5}W_{0·5}O_{6·5}$	2·4 (500)	—0·40[h]	...	pc ; stable in acid	do.
$CdFe_2O_4$	2·3 (550)	—0·10[h]	...	pc ; —	do.
$KTaO_3$[g]	3·5 (370)	—1·25	6% (V_{appl}, 0·25 V, 300 nm)	Xtal ; stable ; $\phi_e = 47\%$ (V_{appl}, 4V ; 254 nm)	Ellis *et al* (1976)
$KTa_{0·77}Nb_{0·23}O_3$	3·6 (390)	—1·35	4% (V_{appl}, 0·25 V)	Xtal ; stable ; $\phi_e = 33\%$ (254 nm)	do.
$Sr_2Nb_2O_7$	3·86	—1·30	0·8% (280 nm ; pH = 8.2) 0·1% (260 nm ; pH = 8.2)	pc ; stable	Hormadaly *et al* (1980)

Table 3—*Contd.*

(1)	(2)	(3)	(4)	(5)	(6)
$Ba_{0.5}Sr_{0.5}Nb_2O_6$	3·38	—0·95	0·04% (280 nm ; pH = 8·2)	stable	do.
$LuRhO_3$	2·20	+0·34	...	Xtal ; stable	Noufi and Tench (1980)
Cd_2SnO_4	2·12	$0·0 \pm 0·10^h$	...	pc ; unstable	Koffyberg and Benko (1980)
$CdIn_2O_4$	2·23	$+0·07 \pm 0·10^h$	...	pc ; stable	do.
Cd_2GeO_3	3·15	$-1·00 \pm 0·10^h$	...	pc ; stable	do.

[a] Data obtained using *n*-SC oxide electrode (unless otherwise specfied as *p*-type) as the photoelectrode in aqueous electrolytes. For widely studied systems only representative data are given. Certain other systems which are qualitatively examined have not been included (for *e.g.*, see, Ruah *et al* 1979).

[b] Electron affinity (EA) and electronegativity (χ) of the SC are given in parenthesis. Values taken from Butler (1977) and Butler and Ginley (1978).

[c] The threshold wavelength for photoresponse (λ_{onset}) in the PEC is given in paranthesis.

[d] E_{fb} is the flat-band potential of the SC determined at pH $\sim$ 13·0 or corrected to this pH suitably employing Nernst equation. More negative value of E_{fb} w.r.t. SCE is desirable to give higher efficiency of photoelectrolysis.

[e] Conversion efficiency, $\eta = \dfrac{\text{(Energy stored as fuel)} - \text{(Electrical energy input)}}{\text{(Incident solar energy)}}$.

For burning of H_2, the maximum recoverable energy from H_2 and $\frac{1}{2}O_2$ is the standard free energy of formation of liquid H_2O, 56 kcal/mol. V_{appl} is the voltage bias applied externally to the cell. Wavelengths of irradiation (λ) are also given. Intensity data generally are not available.

[f] Xtal = single crystal ; pc = polycrystalline. ϕ_e is the quantum efficiency. Wavelength of irradiation is given in parenthesis.

[g] Photoelectrolysis also observed without applied bias in a homogeneous electrolyte (*i.e.*, photoanode and cathode placed in the same solution in a single compartment cell).

[h] Values estimated from current-voltage curves.

Table 4. Double photoelectrode based (*p-n*) photoelectrolysis cells

n-SC/*p*-SC (E_g, eV)	Electrolyte	Energy conversion efficiency, η	Remarks	Reference
n-TiO_2/*p*-GaP (3.0) (2.4)	1 M H_2SO_4 or 1 M NaOH	...	V_{oc} = 580 mV in acid and 400 mV in base. H_2-evolution takes place at *p*-GaP but the cell deteriorates.	Yoneyama *et al* (1975)
n-TiO_2/*p*-GaP	0.2 N H_2SO_4	0.25% (Simulated sunlight from Xe-lamp)	Stable cell operation ; H_2-evolution observed without applied bias.	Nozik (1976, 1977)
n-TiO_2/*p*-GaP	0.2 N H_2SO_4	...	Photochemical diode configuration[a]. Slow evolution of H_2.	do.
n-GaP/*p*-Gap	0.2 N H_2SO_4	...	Corrosion of *n*-GaP.	do.
n-$SrTiO_3$/*p*-GaP (3.2)	1 M NaOH	0.67%	Stable, self driven photoelectrolysis cell	Ohashi *et al* (1977a)
n-$SrTiO_3$/*p*-CdTe (1.4)	1 M NaOH	0.18%	do.	do.
n-TiO_2/*p*-GaP	1 M NaOH	0.1%	do.	do.
n-TiO_2/*p*-CdTe	1 M NaOH	0.04%	do.	do.
n-TiO_2/*p*-$LuRhO_3$ (2.2)	...	0.12%	do.	Jarrett *et al* (1980)

[a] *p-n* type of photochemical diode consists of an *n*-type and a *p*-type sc layer, each of which has an ohmic contact on one side, which are connected together through the ohmic contacts to form a single wafer

with suitable 'catalysts' has been attempted. Effect of thin layers of metals (*e.g.*, Au, Pt, Rh, Ru) deposited on *p*-GaP (Nakato *et al* 1976), *p*-InP (Heller and Vadimsky 1981) have been studied. A photoelectrolysis cell based on surface modified *p*-InP which reaches a solar-to-chemical energy conversion efficiency of 12% (see figure 12) has been recently announced by Heller and Vadimsky (1981). In this cell *p*-InP is coated with a thin layer (100 Å) of Ru and etched in such a way that the SC is anisotropically removed leaving islands of catalytically active metal protected areas and free InP regions. The electrode is further treated to produce a thin oxide layer (monolayer thick) on InP. This cell is the most-efficient one reported so far and it is indeed a breakthrough since in the photo-electrolysis cells reported earlier, the solar conversion efficiencies were disappointingly low (around 1%). The above cell, however, does not have continuous operational capability due to removal of the protective oxide layer on the *p*-InP electrode in the course of operation. Derivatization of SC electrode surfaces with suitable redox reagents (catalysts) is a recent approach to effect H^+-reduction and elimination of photocorrosion at non-oxidic SC's (Wrighton *et al* 1980).

9.2. *Semiconductor/electrolyte liquid junction solar cells*

Several low band gap SC's including Si have been used as photoelectrodes in SC/liquid junction solar cells. Photocorrosion problems with certain SC's have been eliminated by choosing suitable redox electrolytes and surface pretreatments (or modification). Both *n*- and *p*-type SC photoelectrodes are found to give significant energy conversion efficiencies. *n*-GaAs (Parkinson *et al* 1978 a,b) and *n*-WSe_2

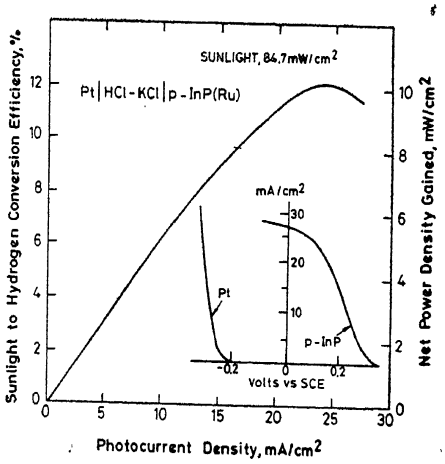

Figure 12. The high efficiency photoassisted water electrolysis cell, Pt/1 M HCl–2M KCl/p-InP(Ru). This cell represents the most efficient (12%) system for the direct conversion of sunlight into the storable fuel, H_2. This cell works under an applied bias. However, the long term stability is yet to be established. Solar-to-hydrogen conversion efficiency and power density gain as a function of photocurrent density are shown. The current-voltage characteristics of a platinum and a *p*-InP (Ru) photocathode at the above sunlight intensity are compared in the inset. With *p*-InP(Ru) photocathode, H_2-evolution starts at $+0{\cdot}36$ V *vs* the SCE or $0{\cdot}64$ V *vs* oxygen electrode. Platinum requires $-0{\cdot}23$ V *vs* SCE or $1{\cdot}23$ V *vs* oxygen (after Heller and Vadimsky 1981).

(Fan *et al* 1980a) electrodes as photoanodes have shown maximum solar-to-electricity conversion efficiencies of 12% (figure 13) and 14% respectively. *p*-InP (Heller *et al* 1981), the first *p*-SC to give high efficiency, has shown an η of 11·5% (figure 14) in aqueous electrolyte. These electrodes have been found to give stable output power over long periods of time with negligible amount of corrosion. As high as 8% conversion efficiency has been reported for slurry-coated polycrystalline electrodes of $CdSe_{0\cdot65}Te_{0\cdot35}$ (Hodes 1980) (figure 15). Even though the presently reported maximum efficiency values are less than those of

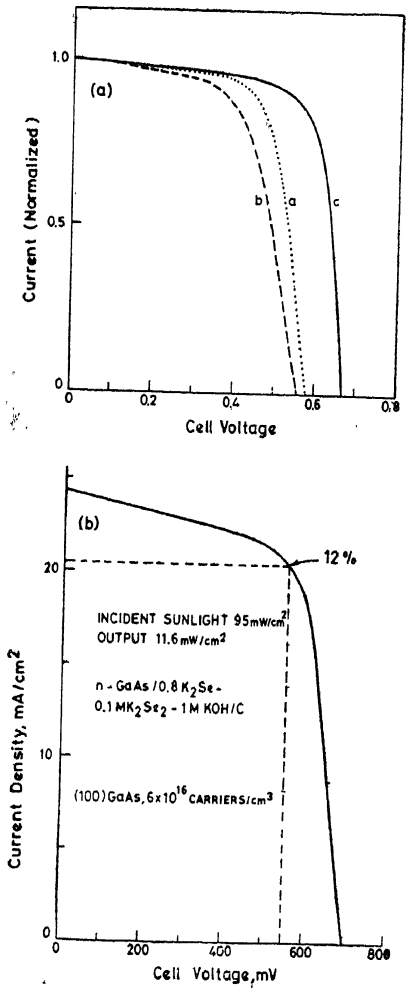

Figure 13. High efficiency (12%) SC/liquid junction (regenerative) solar cell with a photoanode, *n*-GaAs/0·8 M K_2Se–0·1 M K_2Se_2–1 MKOH/C (graphite). (a) Power characteristics of the cell and the changes effected by surface treatment (modification) of *n*-GaAs with Bi^{3+} and Ru^{3+} ions are shown. *Curve* (*a*): Freshly etched electrode (etchant : 1 :1 of 30% H_2O_2–conc. H_2SO_4) followed by dip in the redox couple soln. (I). *Curve* (*b*): I followed by dip in bismuth solution (0·01 M Bi^{3+} + 0·1 M HNO_3). *Curve* (*c*): I followed by dip in ruthenium soln. (0·01 M Ru^{3+} + 0·1 M HNO_3). (b) Same as curve (*c*) of figure 13a with the actual data. As can be seen, Ru^{3+} has beneficial effect. Various other metal ions also have been examined but Ru^{3+} shows the best effect (after Parkinson *et al* 1978a, b).

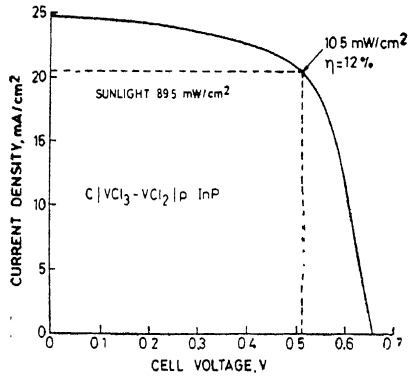

Figure 14. High efficiency (11·5%) SC/liquid junction solar cell with a photocathode, $C/VCl_3 - VCl_2 - HCl/p$–InP. This cell is the first efficient photocathode (p-type SC) based PEC. The p-InP is presumably stabilized against oxidative corrosion by the light-generated electrons arriving at the SC/electrolyte interface. An oxide monolayer or submonolayer on the surface (formed by pretreatment in a mixture of HCl and HNO_3) of the p-InP photocathode prevents electron-hole recombination (after Heller *et al* 1981).

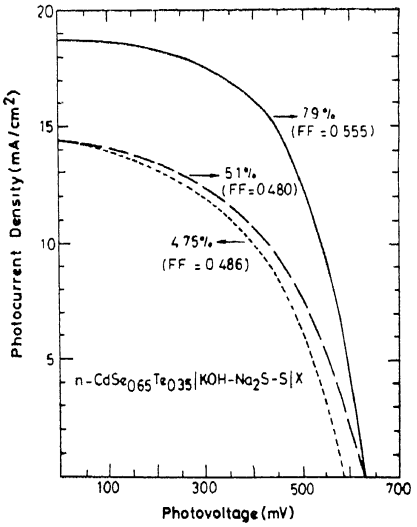

Figure 15. Photocurrent-voltage (power) characteristics of the SC/liquid junction solar cell: n-$CdSe_{0\cdot65}$ $Te_{0\cdot35}$/KOH–Na_2S–S (all 1 M)/X. (X = sulfide impregnated brass gauze). Area of the photoanode, 0·22 cm². Simulated sunlight (0·85 of AM1 radiation). Efficiency and fill factor values are shown. The curves show the effect of etch treatment: dashed curve, HCl : HNO_3 etch; broken curve, CrO_3 etch and K_2CrO_4 treatment; full curve, *photoetch* in the electrolyte followed by treatment with K_2CrO_4 solution (after Hodes 1980).

the corresponding solid state cells (*e.g.*, Si solar cells), it is very encouraging to note that improvements in this area have been much faster, thanks to the well-developed fields of semiconductor technology and electrochemistry. Table 5 gives an account of various PEC's studied for solar-to-electricity conversion.

Table 5. Data on various semiconductors studied in sc-liquid junction solar cells[a]

sc electrode[b] (E_c, eV; λ_{onset}, nm)	Electrolyte[c] (E^0_r V *vs* SCE)	E_{fb}, V *vs* SCE	Light int.[d] mW/cm² (λ, nm)	ϕ_e %[e]	V_{oc}, V[f]	V at[g] η_{max}, V	η_{max}[h]	Reference
(1)	(2)	(3)	(4)	(5)	(6)	(7)	(8)	(9)
n-CdS (Xtal) (2.4 ; 520)	1M NaOH + 1M S + 1M Na_2S (—0.72)	—1.3	0.66 (501.7)	59	...	...	6.8%	Ellis *et al* (1976)
			12 (501.7)	10	...	...	1.7%	do.
			10 (501.7)	...	0.80	...	...	do.
	5M NaOH + 0.09M Na_2Se (69° C) (—0.95)	—1.4	4.4 (501.7)	42	0.42	0.25	3.4%	Ellis *et al* (1977)
	5M NaOH + 0.1M Na_2Te (60° C) (—1.05)	—1.4	1.76 (488)	24	0.40	0.15	...	do.
			90.8 (488)	8	...	0.20	...	do.
	1M NaOH + 1M $Na_2(SCH_2COO)$ + 0.5 M S	—1.36[i]	110 (Hg-lamp, white light)	...	0.60	...	1%	Aruchamy *et al* (1982)
	0.5 M KCl + 0.2M $K_4[Fe(CN)_6]$ + 0.01M $K_3[Fe(CN)_6]$, pH = 11	...	... (Xe-lamp)	70–75 (450–500 nm)	...	...	1.5%	Gerischer (1975)
	0.285M NaI + 3×10^{-4} M I_2 in CH_3CN (+0.3)	—0.8	0.12 (475)	69	1.00	0.7	9.5%	Nakatani *et al* (1978)
n-GaAs (Xtal)/ *n*-CdS (pc)	0.2M NaOH + 0.1M Na_2S + 0.2 M S	...	... (488)	80	1.02 (I_{sc}, 3.75 mA/cm²)	...	2.5% (FF, 0.5)	Wagner and Shay (1977)

Tabel 5—(*Contd.*)

(1)	(2)	(3)	(4)	(5)	(6)	(7)	(8)	(9)
n-CdSe (Xtal) (1.7 ; 750)	1M NaOH + 1M Na_2S + 1M S	—1.43	0.1 (632.8)	52	...	0.35	9.2%	Ellis *et al* (1976)
			2.8 (632.8)	33	...	0.35	6.0%	do.
			10 (514.5)	...	0.65	...	...	do.
			64.6 (sunlight)	...	0.755 (I_{sc}, 9.1 mA/cm²)	0.50	7.1% (FF, 0.5)	Heller *et al* (1978)
	5M NaOH + 0.18M Na_2Se (83° C)	—1.40	6.8 (632.8)	20	0.45	0.20	2.1%	Ellis *et al* (1977)
	5M NaOH + 0.18 M Na_2Te (49° C)	—1.45	24.3 (632.8)	20	0.50	0.15	1.5%	do.
	1 M NaOH + 1 M Na_2S + 1M S + 0·075 M Se	...	64·6 (sunlight)	...	0·765 (I_{sc}, 7·4 mA/cm²)	0·60	6·9% (FF, 0·55)	Heller *et al* (1978)
	1 M NaOH + 1 M $Na_2(SCH_2COO)$ + 0·1M S + 0·1 M Se	—1·42	86·0 (W-lamp, white light)	...	0·600	...	3·5% (FF, 0·30)	Aruchamy *et al* (1982)
	1M NaOH + 1M $Na_2(SCH_2CH_2COO)$ + 0·1M S + 0·2M Se	—1·28[i]	86·0 (W-lamp, white light)	...	0·530	...	3·9% (FF, 0·38)	do.
	0·4 M $Fe(CN)_6^{3-/4-}$ + 0·1 M Et_4NBF_4 in CH_3OH (— 0·08)	—0·9	85·0 (tungsten-halogen lamp)	...	0·72 (I_{sc}, 7 mA/cm²)	0·52	3·2% (FF, 0·56)	Noufi *et al* (1980)
n-CdSe (pc) (Hot pressed)	1 M NaOH + 1 M Na_2S + 1 M S	...	71·0 (sunlight)	...	0·67 (I_{sc}, 12 mA/cm²)	0·45	5·1% (FF, 0·45)	Miller *et al* (1977)

n-CdSe (tf) (anodic oxidation of Cd metal)	1 M NaOH + 1 M Na_2S + 1 M S	...	75·0 (sunlight)	...	0·41 (I_{sc}, 4·6 mA/cm²)	...	0·6% (FF, 0·25)	do.
n-CdSe (tf) (vacuum evaporation)	1 M NaOH + 1 M Na_2S + 1 M S	—1·4	50 (white light)	...	0·50 (I_{sc}, 6·3 mA/cm²)	...	3·9% (FF, 0·61)	Russak *et al* (1980)
n-CdSe (tf) (spray pyrolysis)	1 M NaOH + 1 M Na_2S + 1 M S	...	1 (640) 50 (white light)	... ...	... 0·63 (I_{sc}, 12 mA/cm²)	... ...	7·8% 5·2% (FF, 0·35)	Liu and Wang (1980) do,
n-CdSe (pc) (slurry coated)	1 M KOH + 1 M Na_2S + 1 M S	...	AM 1·5 (sunlight)	...	...	...	3·6% (FF, 0.53)	Tenne and Hodes (1980)
n-$CdSe_{0·65}Te_{0·35}$ (pc) (slurry coated) (1·45 ; 950)	1 M KOH + 1 M Na_2S + 1 M S	...	AM 0·85 (simulated sunlight)	...	0·63	0·45	8·0% (FF, 0·56)	Hodes (1980)
n-CdTe (Xtal) (1·4 ; 865)	5 M NaOH + 0·18 M Na_2Se (49° C)	—1·45	6·8 (632.8)	51	0·70	0·35	9·2%	Ellis *et al* (1977)
	5 M NaOH + 0·18 M Na_2Te	—1·5	1·32 (632.8)	65	0·70	0·30	10·0%	do.
n-$CuInS_2$ (Xtal) (1·53 ; 850)	0–2 M NaOH + 1–2 M Na_2S + 1–3 M S (26–70° C)	...	60–75 (sunlight)	50–60	0·60 (I_{sc}, 21 mA/cm²)	0·3	3·5–4·3% (FF, 0·23–0·31)	Robbins *et al* (1978)
n-GaAs (Xtal) (1·42 ; 930)	5·0 M NaOH + 0·1 M Na_2Te (50° C)	—1·6	32·30 (632·8)	57	0·45	0·2	3·5%	Ellis *et al* (1977)

Table 5 – (*Contd.*)

(1)	(2)	(3)	(4)	(5)	(6)	(7)	(8)	(9)
n-GaAs (Xtal)	1 M KOH + 0·8 M K_2Se + 0·1 M K_2Se_2	...	70 (sunlight)	65	0·65 (I_{sc}, 16·5 mA/cm^2)	0·45	9·0±0·5% (FF, 0·57)	Chang *et al* (1977)
n-GaAs (Xtal) (Ru^{3+} treated surface)	1 M KOH + 0·8 M K_2Se + 0·1 M K_2Se_2	...	95 (sunlight)	65–70	0.70 (I_{sc}, 24 mA/cm^2)	0·55	12% (FF, 0·66)	Parkinson *et al* (1978a, b)
n/n^+ GaAs (Xtal)	1 M KOH + 1 M K_2Se + 0·1 M Se	—1·5[i]	115 (white light)	...	0·70 (I_{sc}, 29 mA/cm^2)	0·65	14% (FF, 0·8)	Noufi and Tench (1980)
n/n^+ GaAs (pc) (molecular beam epitaxy)	1 M KOH + 1 M K_2Se + 0·1 M Se	...	1·5 (white light)	...	0·68 (I_{sc}, 29 mA/cm^2)	0·60	12%	do.
n-GaAs (pc) (CVD) (Ru^{3+} treated surface)	1 M KOH + 0·8 M K_2Se + 0·1M K_2Se_2	...	96·4 (sunlight)	...	0·67 (I_{sc}, 20·3 mA/cm^2)	0·425	7·3% (FF, 0·51)	Heller *et al* (1979)
n-GaAs (Xtal)	1M KCl + 0·07 M $MVCl_2$ + 0·005 M MVCl (aq.) (MV = methyl viologen)	—1·5	... (450W Xe lamp)	...	0·40 (I_{sc}, 1·3 mA/cm^2)	...	... (FF, 0·31)	Fan *et al* (1980b)
n-Si (Xtal) (1·1 ; —)	0·075 M $FeCp_2$ + 1·3 mM $FeCp_2$ + 0·1 M (*n*-Bu_4N) ClO_4 in ethanol ($FeCp_2$ = ferrocene)	—0.4	0·41–4·15 (632·8)	35·38	0·30–0·40	0·20	1·4–2·4%	Legg *et al* (1977)

n-MoS_2 (Xtal) (1·7 ; 800)	1 M $(Et_4N)X/X_2$ in CH_3CN							
	X = Cl (+ 0·84)	...	0·243–4·57 (632·8)	35–53	0.29–0·48	0·12–0·24	1·10–3·75% (FF, 0·15–0·33)	Schneemeyer and Wrighton (1980)
	X = Br (+ 0·48–+ 0·49)	...	0·24–4·6 (632·8)	6–33	0·07–0·24	0·02–0·08	0·08–0·67% (FF, 0·14–0.24)	Schneemeyer and Wrighton (1980)
	X = I (+ 0·04–+ 0·12)	...	0·856–4·6 (632·8)	1	0·03–0·055	0·01–0·02	0·002–0·005% (FF, 0–18–0·22)	do.
	1 M NaI + 0·1 M I_2 (aq.) (+ 0·28)	...	0·242–4·66 (632.8)	16–22	0·34–0·47	0·23–0·33	1·5–2·6% (FF, 0·49–0·53)	do.
n-$MoSe_2$ (Xtal) (1·4 ; —)	1M $(Et_4N)X/X_2$ in CH_3CN							
	X = Cl (+ 0·83–+ 1·05)	+0·32–+ 0·44[i]	0·26–5·9 (632·8)	28–73	0·36–0·55	0·17–0·35	1·2–7·5% (FF, 0·16–0·51)	do.
	X = Br (+ 0·47–+ 0·53)	+ 0·15–+ 0·26[i]	0·3–5·5 (632·8)	8–38	0·29–0·43	0·13–0·15	0·3–1·4% (FF, 0·5–0·29)	do.
	X = I (—0·02–+ 0·085)	—0·1–+ 0·05[i]	0·22–6·4 (632·8)	1–14	0·09–0·19	0·005–0·090	0·02–0·14% (FF, 0·19–0·37)	do.

Table 5—(*Contd.*)

(1)	(2)	(3)	(4)	(5)	(6)	(7)	(8)	(9)
	I_3^-/I^- (aq.)	...	0·26–6·6 (632·8)	20–38	0·36–0·54	0·25–0·33	2–3·9% (FF, 0·29–0·58)	do.
	1 M KI + 0·1 M I_2 (+ 0·28)	—0·3[g]	90 (simulated AM1)	...	0·55 (I_{sc}, 9 mA/cm²)	...	3·5% (FF, 0·67)	Gobrecht *et al* (1978)
	1 M KI + 0·1 M I_2	...	(150W Xe-lamp, 615)	...	0·55 (I_{sc}, 23 mA/cm²)	0·25	4–5% (FF, 0·2–0·25)	Tributsch (1978)
	2 M KI + 0·05 M I_2	...	92·5 (sunlight)	...	0·51 (I_{sc}, 13·2 mA/cm²)	0·33	3·7% (FF, 0·5)	Lawerenz *et al* (1980)
n-WSe) [g]Xtal) (1·35–1·57 ; 930)	1 M NaI + 0·025 M I_3^- + 1 M H^+	—0·45	(150W Xe-lamp, 590)	...	0.71	...	14% (FF, 0·46)	Fan *et al* (1980)
p-GaAs (Xtal)	0·75 M I^- + 0·25 M I_3^- + 1 M H^+	...	1·7 (632·8)	95	0·2 (I_{sc}, 30 mA/cm²)	...	5·6% (FF, 0·65)	Fan and Bard (1980)
	1 M KCl + 0·073 M $MVCl_2$ + 0·005 M MVCl	...	50 (632·8)	13	0·3	...	0·5% (FF, 0·4)	Fan *et al* (1980)
p-InP (Xtal) (1·35 ; —)	0.35 M total (VCl_2—VCl_3) + 4 M HCl (—0·48)	...	110 (sunlight)	...	0·66 (I_{sc}, 25 mA/cm²)	0.52	9·4–11·5% (FF, 0·63)	Heller *et al* (1980, 1981)

p-Si (Xtal) (1·1 ; —)	do.	...	110 (sunlight)	...	0·4 (I_{sc}, 20·4 mA/cm²)	0.18	2·8%	Heller *et al* (1981)
p-MoS_2 (Xtal) (1·7 ; 800)	0·1 M Fe^{2+} + 0·1 M Fe^{3+} + HCl (pH = 1)	...	Xe-lamp (400)	...	0·32 (I_{sc}, 0·1 mA/cm²)	...	0·01–1·0%	Tributsch (1977)
p-WSe_2 (1·35–1·57 ; 930)	1 M H_2SO_4 +0·2 M Fe^{2+}	+0·8–+0·2	130 (Xe-lamp, white light)	40	0·52 (I_{sc}, 21 mA/cm²)	...	2% (FF, 0·23)	Gobrecht *et al* (1978), Kautek and Gerischer (1980)
p-$(CH)_n$ (polyacetylene) (1·5 ; —)	Sodium polysulfide	...	1 (sunlight)	1 (at 2·4 eV)	0·3 (I_{sc}, 0·036 mA/cm²)	...	...	Chen *et al* (1980)

[a] Data obtained using sc electrode as the photoelectrode in aqueous electrolytes. For widely studied systems only representative data are given. Certain other systems which are qualitatively examined have not been included.

[b] Xtal, single crystal ; pc, polycrystalline ; tf, thin film on a suitable substrate. E_g and the threshold wavelength for photoresponse (λ_{onset}) are given in paranthesis.

[c] aq. solution unless otherwise stated ; E^0 is the equilibrium redox potential of the electrolyte.

[d] In most cases a laser (He–Ne or Ar–ion laser) is used for monochromatic illumination. In some cases, white light suitably monochromatized using a monochromater or filters is used.

[e] ϕ_e = quantum efficiency.

[f] V_{oc} is the open circuit photovoltage. I_{sc}, the short circuit current density is given in paranthesis.

[g] V at η_{max} is the output photovoltage of the PEC at the maximum energy conversion efficiency and is useful in calculating the fill factor (FF).

[h] η_{max} is the maximum optical-to-electricity conversion efficiency defined by

$$\eta = \frac{(I \times V)_{max}}{\text{Optical power input}} \times 100$$

where $(I \times V)_{max}$ is the maximum output power of the PEC. Fill factor is given by

$$FF = \frac{(I \times V)_{max}}{I_{sc}.\, V_{oc}}$$ and given in paranthesis.

[i] E_{fb} values estimated from the current-voltage characteristics (photo-onset potentials).

10. Future prospects

Research until now has explored various SC materials for their possible applications in PEC's for solar energy conversion. Essential factors controlling the interfacial processes are fairly well understood. However, crucial materials problems remain to be solved before realizing any practical device. The fact that nearly 50% of the theoretically possible upper limits of energy conversion efficiencies have been achieved with regard to both solar-to-hydrogen (energy storage) and solar-to-electricity conversion in PEC's indicates that further improvements are definitely possible. It is worth noting that the few SC's (*e.g.*, *n*-GaAs, *n*-and *p*-InP) showing high efficiencies satisfy most of the basic solid state characteristics required for photovoltaic device use (see § 6). Further research on similar low band gap materials (both oxidic and non-oxidic) should hold promise in improving the efficiencies further. The manipulation of the interfacial properties of the SC/electrolyte system by suitable surface treatments (etching and surface modifications) is seen as one of the most important factors in improving the performance of a PEC as evidenced by several recent reports. Polycrystalline materials show η's reaching 75% of the single crystal values in PEC's and might prove to be very economical. Cheaper methods of thin film preparation by techniques like CVD, spray pyrolysis, etc., may be attempted. New cell designs to reduce light absorption by solution and internal resistance of the cells are also to be considered in order to improve the overall efficiency. The problems that would arise in large scale photoelectrochemical converters which may include hermetic sealing, collection of products and electrode and electrolyte regeneration are yet unexplored.

In the present discussion on photoelectrolysis more emphasis has been on the decomposition of water. However, in addition to production of H_2 and O_2 other reactions of chemical interest can be driven in a photoelectrochemical cell. Such a cell is generally termed photoelectrosynthesis cell (Bard 1979 ; Calabrese and Wrighton 1981). Photocatalysis is another area of technological importance in which the light energy is used to overcome the energy of activation of a known chemical reaction ($\Delta G < 0$). Cells employing *n*-TiO_2 have been used to carry out the oxidation of CN^-, I^-, acetate, alcohols and a number of organic species (Bard 1979). Heterogeneous photocatalytic systems of this type of 'particulate' systems (*i.e.*, aqueous SC suspensions) may be useful for large scale processes such as water or waste treatment (Bard 1979).

11. Conclusions

In this review, an attempt has been made to briefly review the basic principles of semiconductor photoelectrochemistry. Essential theoretical details pertaining to the photoelectrochemical cells have been outlined. Various problems associated with the SC photoelectrodes in PEC's have been highlighted. Present status of the PEC with a summary of data available on various systems has been given. It is interesting to note that the study of photoelectrochemistry lends itself to diversification in approach with respect to conversion (utilization) of optical energy by

means of PEC's. Recent trends do show that continuous research efforts would give rise to more efficient and viable PEC systems.

Acknowledgement

Thanks are due to Comm. Addl. Sources of Energy CASE, Department of Science and Technology, Govt. of India and CSIR (New Delhi) for the award of research grants.

References

Albery W J and Foulds A W 1979 *J. Photochem.* **10** 41

Alonso N, Beley V M and Chartier P 1981 *Rev. Phys. Appl.* **16** 5

Aruchamy A, Aravamudan G and Subba Rao G V (Unpublished results)

Aruchamy A, Venkatarathnam A, Subrahmanyam M, Subba Rao G V and Aravamudan G 1982 *Electrochim. Acta* **27** 701

Aruchamy A and Wrighton M S 1980 *J. Phys. Chem.* **84** 2848

Bachman K J 1977 in *Semiconductor liquid junction solar cells* (ed.) A Heller (Princeton : Electrochem. Soc.)

Bard A J 1979 *J. Photochem.* **10** 59

Bard A J, Bocarsly A B, Fan F-R F, Walton E G and Wrighton M S 1980 *J. Am. Chem. Soc.* **102** 3671

Bard A J and Kohl P A 1977 *Semiconductor liquid junction solar cells* (ed.) A Heller (Princeton: Electrochem. Soc.) p. 222

Bard A J and Wrighton M S 1977 *J. Electrochem. Soc.* **124** 1706

Becquerel E 1839 *Compt. Rend (Paris)* **9** 561

Bocarsly A B, Bookbinder D C, Dominey R N, Lewis N S and Wrighton M S 1980 *J. Am. Chem. Soc.* **102** 3683

Bockris J O'M and Uosaki K 1976 Energy **1**

Bockris J O'M and Uosaki K 1977a *J. Electrochem. Soc.* **124** 98

Bockris J O'M and Uosaki K 1977b in *Solid state energy conversion and storage* (eds) J B Goodenough and M S Whittingham (Am. Chem. Soc. Adv. Chem. Ser. No. 163)

Bockris J O'M and Uosaki K 1977c *J. Electrochem. Soc.* **124** 1348

Body P J 1968 *J. Electrochem. Soc.* **115** 199

Body P J 1969 *Surface Sci.* **13** 52

Bookbinder D C, Lewis N S, Bradley M G, Bocarsly A B and Wrighton M S 1979 *J. Am. Chem. Soc.* **101** 7721

Brattain W H and Body P J 1966 *Surface Sci.* **4** 18

Brattain W H and Garrett C G B 1955 *Bell Syst. Tech. J.* **34** 129

Butler M A 1977 *J. Appl. Phys.* **48** 1914

Butler M A, Abramovich M, Decker F and Juliao J F 1981 *J. Electrochem. Soc.* **128** 200

Butler M A and Ginley D S 1978 *J. Electrochem. Soc.* **125** 228

Butler M A and Ginley D S 1980 *J. Mater. Sci.* **15** 1

Butler M A, Ginley D S and Eibschutz M 1977 *J. Appl. Phys.* **48** 3070

Butler M A, Nasby R D and Quinn R K 1976 *Solid State Commun.* **19** 1011

Cahen D, Hodes G and Manassen J 1978 *J. Electrochem. Soc.* **125** 375

Calabrese G S and Wrighton M S 1981 *J. Electrochem. Soc.* **128** 1014

Campet G, Dare-Edwards M P, Hamnet A and Goodenough J B 1980 *Nouv. J. de. Chim.* **4** 501

Chang K C, Heller A, Schwartz B, Menezes S and Miller B 1977 *Science* **196** 1097

Chen S N ,Heeger A J, Kiss Z and MacDiarmid A G 1980 *Appl. Phys. Lett.* **36** 96

Clark W D K and Sutin N 1977 *J. Am. Chem. Soc.* **99** 4676

Clechet P, Martin J R, Olier R and Vallouy C 1976 *Compt. Rend. (Paris)* **C282** 887

Dominey R N, Lewis N S and Wrighton M S 1981 *J. Am. Chem. Soc.* **103** 1261

Dutoit E C, Van Mairhaeghe R L, Cardon F and Gomes W P 1975 *Ber. Bunsenges Phys. Chem.* **79** 1206 (and references therein)

Ehrenreich H and Martin J H 1979 *Physics Today*

Ellis A B, Bolts J M, Kaiser S W and Wrighton M S 1977 *J. Am. Chem. Soc.* **99** 2848

Ellis A B, Kaiser S W and Wrighton M S 1976a *J. Am. Chem. Soc.* **98** 1635, 6855

Ellis A B, Kaiser S W and Wrighton M S 1976b *J. Phys. Chem.* **80** 1325

Ellis A B, Kaiser S W and Wrighton M S 1977 *J. Am. Chem. Soc.* **99** 2839

Ellis A B and Karas B R 1979 *J. Am. Chem. Soc.* **101** 236

Ellis A B and Karas B R 1980 *J. Am. Chem. Soc.* **102** 968

Fan F-R F and Bard A J 1980 *J. Am. Chem. Soc.* **102** 3677

Fan F-R F, White H S, Wheeler B and Bard A J 1980a *J. Am. Chem. Soc.* **102** 5142

Fan F-R F, Reichman B and Bard A J 1980b *J. Am. Chem. Soc.* **102** 1488

Fischer C F 1976 in *Festkorper probleme* (Braunschweig : Pergamon) Vol. 14

Frank S N and Bard A J 1975 *J. Am. Chem. Soc.* **97** 7427

Fujishima A and Honda K 1972 *Nature (London)* **238** 37

Fujishima A and Honda K 1975 *J. Electrochem. Soc.* **122** 1487

Gerischer H 1970 in *Physical chemistry* (eds) A H Eyring, D Henderson and W Jost (New York : Academic Press) Vol. 9

Gerischer H 1975 *J. Electroanal. Chem.* **58** 263

Gerischer H 1977a *J. Electroanal. Chem.* **82** 133

Gerischer H 1977b in *Semiconductor liquid junction solar cells* (ed.) A Heller (Princeton : Electrochem. Soc.)

Gerischer H 1979 in *Topics in applied physics.* Vol. 31. Solar energy conversion (ed.) B O Seraphin (Berlin : Springer-Verlag)

Gerischer H and Willig F 1976 in *Topics in current chemistry* (Berlin : Springer-Verlag)

Ghosh A K and Maruska H P 1977 *J. Electrochem. Soc.* **124** 1516

Ginley D S and Butler M A 1977 *J. Appl. Phys.* **48** 2019

Gobrecht J, Gerischer H and Tributsch H 1978a *Ber. Bunsenges Phys. Chem.* **82** 1331

Gobrecht J, Tributsch H and Gerischer H 1978b *J. Electrochem. Soc.* **125** 2085

Goodenough J B, Hamnett A, Dare-Edwards M P, Campet G and Wright R D 1980 *Surface Sci.* **101** 531

Gourgaud S and Elliot D 1977 *J. Electrochem. Soc.* **124** 102

Green M 1959 in *Modern aspects of electrochemistry* (ed.) J O M Bockris (London: Butterworths) Vol. 2, p. 343

Hamnet A, Dare-Edwards M P, Wright R D, Seddon K R and Goodenough J B 1980 *J. Phys. Chem.* **83** 3280

Hardee K L and Bard A J 1977 *J. Electrochem. Soc.* **124** 215

Harris L A, Cross D R and Gerstner M E 1977 *J. Electrochem. Soc.* **124** 839

Harris L A and Wilson R H 1976 *J. Electrochem. Soc.* **123** 1010

Harris L A and Wilson R H 1978 *Annu. Rev. Mater. Sci.* **8** 99

Heller A 1980 in *Photoeffects at semiconductor-electrolyte interfaces* (ed.) A J Nozik (Am. Chem. Soc. Adv. Chem. Ser. No. 180), p. 215

Heller A and Vadimsky R G 1981 *Phys. Rev. Lett.* **46** 1153

Heller A, Miller B and Thiel F A 1981 *Appl. Phys. Lett.* **38** 282

Heller A, Miller B, Chu S S and Lee Y T 1979 *J. Am. Chem. Soc.* **101** 7633

Heller A, Schwartz G P, Vadimsky A G, Menezes S and Miller B 1978 *J. Electrochem. Soc.* **125** 1156

Heller A, Miller B, Lawerenz H J and Bachman K J 1980 *J. Am. Chem. Soc.* **102** 6555

Heller A, Lawerenz H J and Miller B 1981 *J. Am. Chem. Soc.* **103** 200

Hodes G 1980 *Nature (London)* **285** 29

Hodes G, Manassen J and Cahen D 1976 *Nature (London)* **261** 403

Hormadaly J, Subbarao S N and Wold A 1980 *J. Solid. State Chem.* **33** 27

Houlihan J F, Armitage D B, Hoovler T, Bonaquist D, Madacsi D P and Mulay L N 1978 *Mat. Res. Bull.* **13** 1208

Houlihan J, Hamilton J R and Madacsi D P 1979 *Mat. Res. Bull.* **14** 915

Hovel H J 1975 in *Semiconductors and semimetals* (New York: Academic Press) Vol. **11**

Inoue T, Watanabe T, Fujishima A, Honda K and Kohayakawa K 1977 *J. Electrochem. Soc.* **124** 719

Jarrett H S, Sleight A W, Kung H H and Gillson J L 1980 *J. Appl. Phys.* **51** 3916

Johnston W D, Leamy H J, Parkinson B A, Heller A and Miller B 1980 *J. Electrochem. Soc.* **127** 90

Kautek W and Gerischer H 1980 *Ber. Bunsenges Phys. Chem.* **84** 645

Koffyberg F P and Benko F A 1980 *Appl. Phys. Lett.* **37** 320

Kohl P A and Bard A J 1978 *J. Electrochem. Soc.* **125** 375

Kohl P A, Frank S N and Bard A J 1977 *J. Electrochem. Soc.* **124** 225

Kung H H, Jarrett H S, Sleight A W and Ferreetti A 1977 *J. Appl. Phys.* **48** 2463

Laser D and Gottesfeld S 1979 *J. Electrochem. Soc.* **126** 475

Lawerenz H J, Heller A and DiSalvo F J 1980 *J. Am. Chem. Soc.* **102** 1877

Legg K D, Ellis A B, Bolts J M and Wrighton M S 1977 *Proc. Natl. Acad. Sci. USA* **74** 4116

Liu C-H J and Wang J H 1980 *Appl. Phys. Lett.* **36** 852

Loferski J J 1956 *J. Appl. Phys.* **27** 777

Lohmann F 1967 *Z. Naturforsch.* **A22** 843

Matsumura M, Nomura Y and Tsubomura H 1977 *Bull. Chem. Soc. Jpn.* **50** 2533

Mavroides J G 1977 in *Semiconductor liquid junction solar cells* (ed.) A. Heller (Princeton: Electrochem. Soc.) p. 84

Mavroides J G 1978 *Mat. Res. Bull.* **13** 1379

Mavroides J G and Kolesar D F 1978 *J. Vac. Sci. Technol.* **15** 538

Mavroides J G, Kafalas J A and Kolesar D F 1976 *Appl. Phys. Lett.* **28** 241

Mavroides J G, Tchernev D I, Kafalas J A and Kolesar D F 1975 *Mat. Res. Bull.* **10** 1023

Memming R 1964 *Philips. Res. Rep.* **19** 323

Memming R 1978–79 *Philips Tech. Rev.* **38** 160

Memming R 1980 *Electrochim. Acta* **25** 77

Memming R and Schroppel F 1979 *Chem. Phys. Lett.* **62** 207

Memming R, Schroppel F and Bringmann U 1979 *J. Electroanal. Chem.* **100** 307

Metikos-Hukovic M and Lovrecek B 1978 *Electrochim. Acta* **23** 1371

Miller B and Heller A 1976 *Nature (London)* **262** 680

Miller B, Heller A, Robbins M, Menezes S, Chang K C and Thomson J Jr 1977a *J. Electrochem. Soc.* **124** 1019

Miller B, Menezes S and Heller A 1977b in *Semiconductor liquid junction solar cells* (ed.) A Heller (Princeton: Electrochem. Soc.)

Morisaki H, Watanabe T, Iwase M and Yazawa K 1976 *Appl. Phys. Lett.* **29** 338

Myamlin V A and Pleskov Yu V 1967 *Electrochemistry of semiconductors* (New York: Plenum)

Nakatani K, Matsudaira S and Tsubomura H 1978 *J. Electrochem. Soc.* **125** 406
Nakato Y, Tsubomura H and Tonomura S 1976 *Ber. Bunsenges Phys. Chem.* **80** 1289
Noufi R, Kohl P A, Rogers J W Jr, White J M and Bard A J 1979 *J. Electrochem. Soc.* **126** 949
Noufi R and Tench D 1980 *J. Electrochem. Soc.* **127** 188
Noufi R, Tench D and Warren L F 1980 *J. Electrochem. Soc.* **127** 2709
Nozik A J 1976a *Appl. Phys. Lett.* **29** 150
Nozik A J 1976b *Proc. 11th Intersoc. Energy Conv. Eng. Conf.* Nevada p. 43
Nozik A J 1977a *Appl. Phys. Lett.* **30** 567
Nozik A J 1977b *J. Cryst. Growth* **39** 200
Nozik A J 1978 *Annu. Rev. Phys. Chem.* **29** 189
Ohashi K, McCann J and Bockris J O' M 1977a *Nature (London)* **266** 610
Ohashi K, Uosaki K and Bockris J O' M 1977b *Energy Res.* **1** 25
Parkinson B A, Heller A and Miller B 1978a *Conf. Rec. IEEE Photovoltaic Spec. Conf.* **13** 1253
Parkinson B A, Heller A and Miller B 1978b *Appl. Phys. Lett.* **33** 521
Quinn R K, Nasby R D and Baughman R J 1976 *Mat. Res. Bull.* **11** 1011
Rajeshwar K, Singh P and DuBow J 1978 *Electrochim. Acta* **23** 1117
Robbins M, Bachman K J, Lambrecht V G, Thiel F A, Thomson J Jr., Vadimsky R G, Menezes S, Heller A and Miller B 1978 *J. Electrochem. Soc.* **125** 831
Ruah R D, Buzby J M, Reise J F and Alkaitis S A 1979 *J. Phys. Chem.* **83** 2221
Russak M A, Reichman J, Witzke H, Deb S K and Chen S N 1980 *J. Electrochem. Soc.* **127** 725
Sayers C N and Armstrong N R 1978 *Surface Sci.* **77** 301
Schneemeyer L F and Wrighton M S 1980 *J. Am. Chem. Soc.* **102** 6964
Sze S M 1969 *Physics of semiconductor devices* (New York : John Wiley)
Tenne R and Hodes G 1980 *Appl. Phys. Lett.* **37** 428
Tomkiewicz M and Fay H 1979 *Appl. Phys.* **18** 1
Tomkiewicz M and Woodall J M 1977 *J. Electrochem. Soc.* **124** 1348
Tributsch H 1977a *Z. Naturforsch.* **A32** 972
Tributsch H 1977b *Ber. Bunsenges. Phys. Chem.* **81** 361
Tributsch H 1978 *J. Electrochem. Soc.* **125** 1086
Tributsch H and Bennett J C 1977 *J. Electroanal. Chem.* **81** 91
Tsubomura H, Matsumura M, Nomura Y and Amamiya T 1976 *Nature (London)* **261** 402
Turner J A, Manassen J and Nozik A J 1980 *Appl. Phys. Lett.* **37** 488
Wagner S and Shay J L 1977 *Appl. Phys. Lett.* **31** 446
Watanabe T, Fujishima A and Honda K 1976 *Bull. Chem. Soc. Jpn* **49** 355
Watanabe T, Nakato M, Fujishima A and Honda K 1980 *Ber. Bunsenges. Phys. Chem.* **84** 74
Williams R 1960 *J. Chem. Phys.* **32** 1505
Wrighton M S 1979 *Acc. Chem. Res.* **12** 303
Wrighton M S, Bocarsly A B, Bolts J M, Bradley M G, Fischer A B, Lewis N S, Palazzotto M C and Walton E G 1980 in *Advances in chemistry* Ser. No. **184** (ed.) M S Wrighton (Am. Chem. Soc.) p. 270 (and references therein)
Wrighton M S, Ellis A B, Wolczanski P T, Morse D L, Abrahamson H B and Ginely D S 1976 *J. Am. Chem. Soc.* **98** 2774
Wrighton M S, Ginley D S, Wolczanski P T, Ellis A B, Morse D L and Linz A 1975 *Proc. Natl. Acad. Sci. USA* **72** 1518
Wrighton M S, Morse D L, Ellis A B, Ginley D S and Abrahamson H B 1976 *J. Am. Chem. Soc.* **98** 44
Wrighton M S, Austin R G, Bocarsly A B, Bolts J M, Hass O, Legg K D, Nadjo L and Palazzotto M C 1978 *J. Am. Chem. Soc.* **100** 1602
Yamase T, Gerischer H, Lubke M and Pettinger B 1979 *Ber. Bunsenges. Phys. Chem.* **83** 658
Yoneyama H, Sakamoto H and Tamura H 1975 *Electrochim. Acta* **20** 341